University Library

MINERVA ACCESS

A gateway to Melbourne's research publications

Minerva Access is the Institutional Repository of The University of Melbourne

Author/s:
Krátký, J;Zajíčková, M;Taki, AC;Michel, O;Matoušková, P;Vokřál, I;Štěrbová, K;Vosála, O;Lungerich, B;Kurz, T;Gasser, RB;Harant, K;Skálová, L

Title:
New derivatives of benzhydroxamic acid with nematocidal activity against Haemonchus contortus and Caenorhabditis elegans

Date:
2025-08-01

Citation:
Krátký, J., Zajíčková, M., Taki, A. C., Michel, O., Matoušková, P., Vokřál, I., Štěrbová, K., Vosála, O., Lungerich, B., Kurz, T., Gasser, R. B., Harant, K. & Skálová, L. (2025). New derivatives of benzhydroxamic acid with nematocidal activity against Haemonchus contortus and Caenorhabditis elegans. International Journal for Parasitology Drugs and Drug Resistance, 28, pp.100599-. https://doi.org/10.1016/j.ijpddr.2025.100599.

Persistent Link:
https://hdl.handle.net/11343/360797

License:
CC BY-NC-ND

International Journal for Parasitology: Drugs and Drug Resistance 28 (2025) 100599

Contents lists available at ScienceDirect

International Journal for Parasitology: Drugs and Drug Resistance

journal homepage: www.elsevier.com/locate/ijpddr

New derivatives of benzhydroxamic acid with nematocidal activity against *Haemonchus contortus* and *Caenorhabditis elegans*

Josef Krátký [a], Markéta Zajíčková [a], Aya C. Taki [b], Oliver Michel [c], Petra Matoušková [a], Ivan Vokřál [d], Karolína Štěrbová [a], Ondřej Vosála [a], Beate Lungerich [c], Thomas Kurz [c], Robin B. Gasser [b], Karel Harant [e], Lenka Skálová [a,*]

[a] Department of Biochemical Sciences, Faculty of Pharmacy, Charles University, Hradec Králové, Czech Republic
[b] Department of Veterinary Biosciences, Melbourne Veterinary School, The University of Melbourne, Parkville, Victoria, 3010, Australia
[c] Institute of Pharmaceutical and Medicinal Chemistry, Heinrich-Heine University, Düsseldorf, Germany
[d] Department of Pharmacology and Toxicology, Faculty of Pharmacy, Charles University, Hradec Králové, Czech Republic
[e] Laboratory of Mass Spectrometry, BIOCEV, Faculty of Science, Charles University, Vestec u Prahy, Czech Republic

ARTICLE INFO

Keywords:
Drug development
Drug resistance
Nematodes
New anthelmintics

ABSTRACT

Parasitic nematodes cause a wide range of diseases in animals, including humans. However, the efficacy of existing anthelmintic drugs, commonly used to treat these infections, is waning due to the increasing prevalence of drug resistance in nematode populations. This growing challenge underscores the urgent need to discover and develop novel nematocidal drugs that target new molecular pathways. In the present study, 13 novel derivatives of benzhydroxamic acid (OMKs) were designed and synthesized. Their anthelmintic activity was tested in the parasitic nematode *Haemonchus contortus* (barber's pole worm) and the free-living nematode *Caenorhabditis elegans* and potential toxicity assessed in mammalian models. Compound OMK211 showed the most promising results. It decreased viability and motility of larval and adult stages of both nematode species and of both drug-sensitive and drug-resistant strains of *H. contortus* at micromolar concentrations with the highest efficacy in *H. contortus* adult males ($IC_{50} \sim 1$ μM). Moreover, OMK211 was not toxic in mammalians cells *in vitro* and in mice *in vivo*. Consequently, thermal proteome profiling analysis was used to infer the putative molecular target of OMK211 in *H. contortus*. The results revealed C2-domain containing protein A0A6F7Q0A8, encoded by gene HCON_00184,900, as an interacting partner of OMK211. Using advanced structural prediction and docking tools, this protein is considered an interesting putative molecular target of new nematocidal drugs as its orthologs are present in several nematodes but not in mammals. In conclusion, novel derivatives of benzhydroxamic acid represent a promising new class of potential anthelmintics, which deserve further testing.

1. Introduction

Anthelmintic drugs continue to play a crucial role in the treatment and control of nematode infections. However, the excessive and sub-optimal usage of drugs has led to the emergence of anthelmintic resistance in nematodes to major classes (including benzimidazoles, imidazothiazoles, macrocyclic lactones, and the amino-acetonitrile derivative monepantel) (Mukherjee et al., 2023; Cai et al., 2024; Ng'etich et al., 2024; Pramanik et al., 2024). Resistance has been observed particularly in nematode species of livestock animals (order Strongylida; family Trichostrongylidae) (Klauck et al., 2014; Kotze and Prichard, 2016). Representing this family, *Haemonchus contortus* (the barber's pole worm) is one of the most extensively studied parasitic nematodes (Kotze and Prichard, 2016; Rychlá et al., 2024). However, free living nematode *Caenorhabditis elegans* is a widely-used model nematode both for testing potential nematocidal compounds and for uncovering mechanisms of drug resistance (Hahnel et al., 2020; Piao et al., 2020; Brinzer et al., 2024; Shanley et al., 2024).

H. contortus is the causative agent of haemonchosis, a parasitic disease predominantly of small ruminants (e.g., sheep and goats). This disease manifests as anaemia, oedema (e.g., bottle jaw or ascited), weakness and weight loss, and, in cases, and can lead to death of the

* Corresponding author. Dept. of Biochemical Sciences, Faculty of Pharmacy, Charles University, Heyrovského 1203, EU, CZ-500 05, Hradec Králové, Czech Republic.
E-mail address: lenka.skalova@faf.cuni.cz (L. Skálová).

https://doi.org/10.1016/j.ijpddr.2025.100599
Received 29 January 2025; Received in revised form 12 May 2025; Accepted 18 May 2025
Available online 20 May 2025
2211-3207/© 2025 The Authors. Published by Elsevier Ltd on behalf of Australian Society for Parasitology. This is an open access article under the CC BY-NC-ND license (http://creativecommons.org/licenses/by-nc-nd/4.0/).

animal. (Arsenopoulos et al., 2021). The life cycle and transmission dynamics of *H. contortus* are significantly influenced by climatic conditions. This parasite thrives in warm and humid environments, with subtropical to tropical climates offering optimal conditions for its development and infection in ruminant hosts. However, *H. contortus* has remarkable adaptability, enabling it to persist in temperate, cold and even arid regions, highlighting its resilience and capacity to exploit diverse ecological niches (Veglia, 1915). Thus, global change could lead to altered or increased transmission patterns of *H. contortus* infection and haemonchosis (Silverman and Campbell, 1959; Salle et al., 2019; Ahmad et al., 2024).

The economic impact of haemonchosis is substantial, with decreased farm productivity leading to significant financial losses (Gasser et al., 2008; McRae et al., 2014). Furthermore, the costs associated with anthelmintic treatment, diagnosis and management represent additional financial burdens linked to the control of haemonchosis and related trichostrongylid nematodes (Lanusse et al., 2018). For instance, the costs of treatment in India and South Africa were estimated at US$ 100 million and US$ 46 million, respectively (Arsenopoulos et al., 2021). Control efforts are further complicated by the existence of *H. contortus* strains that are resistant to most commercially available anthelmintic drugs (Taman and Azab, 2014; Kotze and Prichard, 2016). Notably, resistance to monepantel within two years of its introduction to the market (Sales and Love, 2016) is a stark reminder of the adverse impact of anthelmintic resistance on nematode control in livestock animals.

Thus, there is major demand for the discovery and development of novel anthelmintics (Preston et al., 2016; Zajíčková et al., 2020). Discovery relies on two main screening approaches: target-based, which involves assays for function or binding with pathogen proteins in isolation, and phenotype-based, which screens for bioactive compounds that alter the phenotype of the organism. Phenotypic screening is particularly promising because it can identify compounds with novel targets and mechanisms of action (Nguyen et al., 2019).

Using a phenotype-based approach, we recently screened 236 chemically-diverse compounds from the "Kurz-box" library (a small compound library containing heterocyclic compounds, hydroxamic acid-based metalloenzyme inhibitors, peptidomimetics and various synthesis intermediates formed by T. Kurz and B. Lungerich at Heinrich-Heine-University) and identified a benzhydroxamic acid derivative – designated BLK127 – as a promising molecule with activity against exsheathed third- (xL3) and fourth-stage (L4) larvae of *H. contortus* (Nguyen et al., 2019). Compound BLK127 induced an eviscerated phenotype, characterised by a pronounced protrusion of internal tissues and organs through the excretory pore in xL3s, and significantly inhibited L4 development after seven days of incubation *in vitro* (Nguyen et al., 2019). BLK127 also significantly reduced the viability of *H. contortus* adults and did not exhibit hepatotoxicity *in vitro* (Zajíčková et al., 2022).

Logically extending previous work, the aims of the present study were to (i) design and synthesise a series of benzhydroxamic acid derivatives (designated as OMKs); (ii) evaluate these OMKs in *H. contortus* and *C. elegans* and (iii) assess the toxicity of promising OMKs in mammalian models; and (iv) infer the possible molecular target(s) of the most promising OMK derivative in *H. contortus* adults using thermal proteome profiling.

2. Material and methods

2.1. Reagents and chemicals

ATP Bioluminescence assay kit CLS II, was purchased from Roche, Mannheim, Germany. The Pierce™ BCA Protein Assay Kit, TMT10plex™ Isobaric Label reagents and kits (90,110), Roswell Park Memorial Institute 1640 medium (RPMI-1640) with no phenol red (11835030), Dulbecco's modified Eagle medium (DMEM; 11965092), GlutaMax™ (35050061), foetal bovine serum (FBS), antibiotic-antimycotic (15240062) were purchased from Thermo Fisher Scientific (Czech Republic and Australia). RPMI-1640 (R8758) and all other chemicals were purchased from Sigma-Aldrich (Prague, Czech Republic). Commercial anthelmintics including monepantel (Zolvix™; Elanco, USA) and moxidectin (Cydectin®; Virbac, France) were purchased from respective manufacturers.

2.2. Synthesis of OMK compounds

The design of novel benzhydroxamic acid derivatives (named OMKs) was based on the structure of BLK127. The structures and synthesis of all OMK compounds is presented in Fig. 1. Generally, 2.0 mmol of the appropriate carboxylic acid **1a-c** were dissolved at room temperature together with 2.4 mmol of *O*-(7-azabenzotriazol-1-yl)-*N,N,N′,N′*-tetramethyluronium hexafluorophosphate (HATU) and 6.0 mmol of *N,N*-diisopropylethylamine in 10 mL anhydrous *N,N*-dimethylformamide. After stirring for 10 min, 2.2 mmol of the respective O-substituted hydroxylamine hydrochloride **2a-k** was added, and the mixture was stirred for an additional 16 h at room temperature. After complete conversion determined by TLC, the solvent was removed under reduced pressure. The residue was dissolved in 15 ml deionized water and extracted three times with 20 ml ethyl acetate. The combined organic layers were washed with saturated sodium chloride solution and dried over anhydrous sodium sulphate. After filtration and solvent removal, the crude product was purified by column chromatography on silica gel using *n*-hexane/ethyl acetate as eluent mixture. Finally, all OMK compounds were recrystallized from *n*-hexane/ethyl acetate. The description of individual OMK synthesis and their precise characterization (^{1}H-NMR,^{13}C-NMR, HPLC, melting point, HRMS) is presented in Suppl. 1.

2.3. Purity and chemical stability of OMK compounds

At pH 7.4 compound OMK dissolved in a mixture of Tween20/ethanol/phosphate buffer pH 7.4 (7/3/90) upon shaking (300 rpm) shaken for 48 h 24 °C. The chemical stability was monitored over 48 h at 0 h, 1 h, 3 h, 6 h, 24 h and 48 h by a Knauer HPLC system combined with a KNAUER UV Detector Azura UVD 2.1L. Column KNAUER Eurospher II 100-5 C18, 150 × 4 mm, mobile phase 1 (linear gradient (90−0 %) of water with 0.1 % of trifluoroacetic acid) and mobile phase 2 (linear gradient (10–100 %) of acetonitrile with 0.1 % of trifluoroacetic acid) were used. Run time was 20 min, followed by an isocratic elution with 100 % acetonitrile for 10 min. Injection volume 10 µl and flow rate 1.00 ml/min were used. Detection was set up at 254 nm.

2.4. Experimental animals

The animal experiments were conducted in accordance with the Guide for the Care and Use of Laboratory Animals (Protection of Animals from Cruelty Act No. 246/92, Czech Republic) and the Australian Code for the Care and Use of Animals for Scientific Purposes (National Health and Medical Research Council, Australia). All procedures are also in accordance with Directive 2010/63/EU on the protection of animals used for scientific purposes. The breeding facilities in the Czech Republic were accredited by the Ministry of Agriculture of the Czech Republic for experimental sheep housing (Approval MZE-53255/2022–13143) and rodent housing (Approval MZE-66298/2023–13143). All experimental procedures involving sheep and mice were evaluated and approved by the Ethics Committee of the Ministry of Education, Youth and Sports of the Czech Republic (sheep for worms and liver - project number MSMT-20144/2023–4; mice toxicity testing – project number MSMT-16321/2022–3) or in accordance with the Institutional Animal Ethics Guidelines (permit no. 23983; University of Melbourne) and Australian regulations.

Prior to the isolation of the *H. contortus* or the liver, sheep were sacrificed using a captive bolt pistol and exsanguinated to confirm death. Mice were sacrificed under general isoflurane anaesthesia by

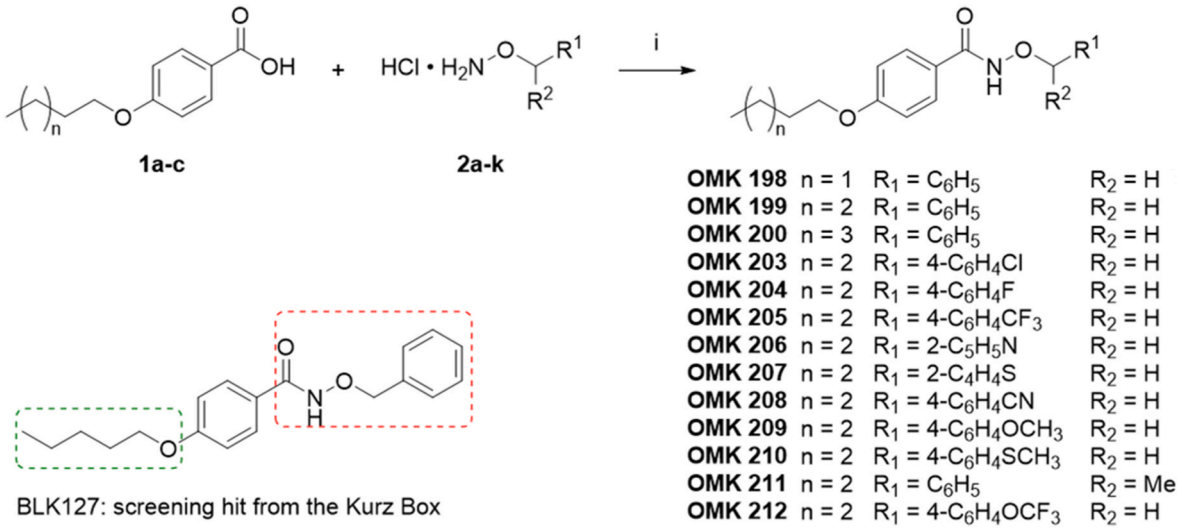


Fig. 1. Structure of the original compound BLK127 and the scheme of synthesis and structures of novel derivatives OMK198-212. See Suppl. 1 for details.

cervical dislocation. These procedures are in accordance with Annexe IV of Directive (2010)/63/EU and national legislation of the Czech Republic and Australia.

2.5. Production of H. contortus

Three strains of *H. contortus* were used: the ISE strain (Inbred-Susceptible-Edinburgh, MHco3; Roos et al., 2004), which is susceptible to all classes of anthelmintics, WR (White-River; MHco4; van Wyk and Malan, 1988; Redman et al., 2008), a multidrug resistant strain (Yilmaz et al., 2017; Raisová Stuchlíková et al., 2018) and the Haecon-5 strain (Schwarz et al., 2013; Zheng et al., 2024). All lambs were dewormed with single dose of albendazole (*per os* 5 mg/kg) or a combination of moxidectin (*per os* 0.2 mg/kg) and monepantel (*per os* 0.1 mg/kg). For ISE and WR strains, six parasite-free male sheep (Texel breed, six-months-old) were orally infected with 8000 L3s (suspended in 5 ml of water) of *H. contortus*. For the Haecon-5 strain, two parasite-free male sheep (Merino breed, six-months-old) were orally inoculated with 7000 L3s (suspended in 50 ml of water) of *H. contortus*.

2.6. Isolation of H. contortus eggs

Five weeks after the infection of the sheep with *H. contortus*, the faeces were collected (twice a day for three consecutive days) and transported in plastic bags to the laboratory. There, the faeces were homogenized with tap water. The eggs were isolated using a system of three sieves of varying sizes (250, μm, 100 μm, and 25 μm), respectively. The contents of the last sieve with the smallest size (25 μm) were removed and centrifuged at 1600×*g* for 3 min in Falcon tubes. After the removal of the supernatant, the volume was replenished with a flotation solution of sucrose (1.27 g cm^{-3}) and the samples were centrifuged at 1000×*g* for 3 min. Subsequently, the eggs were washed and centrifuged at 1600×*g* for 3 min. This process was repeated until the egg suspensions were clear, with the final step being verified microscopically. The number of eggs was counted using a microscope at 40-times magnification and they were stored at 4 °C.

2.7. Procurement of H. contortus larvae

Four weeks after infection, faecal samples containing *H. contortus* eggs were collected from sheep with patent infection daily. *H. contortus* L3s were produced from eggs by incubating these faecal samples at 27 °C and >90 % relative humidity for seven days, and collected in tap water and sieved through two layers of nylon mesh (pore size: 20 μm; Rowe Scientific, Australia) to remove debris or dead larvae, and then stored (at a concentration of 2000 L3s per ml) at 11 °C for up to six months (cf. Preston et al., 2015). Immediately prior to screening, L3s were artificially exsheathed via exposure to 0.15 % (v/v) sodium hypochlorite at 38 °C for 20 min with gentle shaking (Taki et al., 2021). Following this treatment, exsheathed L3s (xL3s) were immediately washed five times in 50 ml of sterile saline by centrifugation at 500×*g* (5 min) at room temperature (22–24 °C). After the last wash, xL3s were suspended in sterile lysogenic broth (LB) (Bertani, 1951) supplemented with 100 IU/ml of penicillin, 100 μg/ml of streptomycin and 0.25 μg/ml of amphotericin B – LB* (Thermo Fisher Scientific, USA).

2.8. Isolation of H. contortus adults

The sheep have been euthanized by a veterinarian according to the protocols in force as described in Chapter 2.4. Adult worms were collected from the abomasum at necropsy (7 weeks after inoculation) using an agar method (Kellerová et al., 2020), and male and female worms separated using a dissection microscope. Adult worms were washed several times in phenol-red free RPMI 1640 medium supplemented with 100 IU/ml of penicillin, 100 μg/ml of streptomycin and 0.25 μg/ml of amphotericin B (designated RPMI*) and used immediately for the assay.

2.9. Egg hatch test (EHT) in H. contortus

Fresh *H. contortus* eggs were suspended in water and incubated in 96-well plates with OMK derivatives (concentration range of 0–50 μM), with a final volume of 200 μL and containing 50 eggs per well. The OMKs were pre-dissolved in DMSO, with the final concentration of DMSO of 0.5 % (*v/v*) in each tested concentration. An egg suspension with 0.5 % (*v/v*) DMSO only was utilized as a negative control, while a solution of thiabendazole at concentrations of 25, 12.5, 6.25, 3.12, 1.56, 0.78, 0.39, and 0.19 μM was employed as a positive control. The 48-h incubation period at 27 °C was terminated by the addition of 5 μl of Lugol's solution. The egg/larvae ratio was assessed through microscopic examination.

2.10. Motility and larval development test in H. contortus xL3

The dose-response assay for *H. contortus* followed a well-established protocol (Taki et al., 2021). Test compounds were assessed individually for an effect on the motility of xL3s (10-points, 2-fold serial dilution in) LB*, concentration range of 0.4–100 μM). Monepantel and moxidectin

(prepared in the same manner as the test compounds), were used as positive controls. A solution of LB* was used as a negative control. The test compounds and positive control compounds were arrayed in triplicate across individual flat-bottom 96-well microplates, with six wells on each plate containing the negative control. Added to each well were 300 xL3s of *H. contortus* in 50 µl of LB* to give a final volume of 100 µl. Plates were then placed in a CO_2 incubator (10 % [*v/v*] CO_2, 38 °C, >90 % humidity). After 90 h of incubation, worm activity was captured using a WMicroTracker ONE unit (Phylumtech, Argentina). Over a period of 15 min, disturbance of an infrared beam in individual wells was recorded as a worm activity count. Raw 'activity counts' for each well were normalized to the negative controls. The compound concentrations were log_{10}-transformed and fitted using a variable slope four-parameter equation, using the ordinary least squares fit model, employing Prism (v.10.3.1 GraphPad Software, San Diego, CA, USA). Larval development was established at 168 h of incubation with compound, as described previously (Preston et al., 2015). The development inhibition and phenotypes of larvae were examined using a microscope (Preston et al., 2015). Any non-wildtype (abnormal) phenotypes exhibited by the larvae were recorded (Taki et al., 2021).

2.11. Motility test of H. contortus adults

The activity of OMK207 and OMK211 was assessed on adult females of *H. contortus* in an established assay (Taki et al., 2020). The compound was added in triplicate to the wells of a 24-well plate (cat. no. 3524; Corning, USA) at a concentration of 100 µM in 500 µL of RPMI. Two positive-control compounds, monepantel and moxidectin, and a negative control containing 1 % (*v/v*) DMSO only, were included in triplicates on the same plate. Four adult females were added to each of the triplicate wells containing either the test compound or the controls and placed in a CO_2 incubator (10 % [*v/v*] CO_2, 38 °C, >90 % relative humidity) for 24 h. A video recording (30 s) of each well was taken at 0 h, 1 h, 3 h, 5 h and 24 h during the total incubation period to assess the reduction in worm motility, which was scored as 3 ("good"), 2 ("low"), 1 ("very low") or 0 ("no movement"; cf. Taki et al., 2020). For each test or control compound, the motility scores for each of the triplicate wells were calculated, normalized with reference to the negative control (100 % motility) and recorded as a percentage.

2.12. Viability test in H. contortus adults

The effect of OMK derivatives on the viability of adult *H. contortus* males and females was assessed through the quantification of ATP, which serve as an indicator of viability. The methodology and underlying principles were previously described in detail (Zajíčková et al., 2021). In brief, males (16 in one well) and females (8 in one well) of *H. contortus* were incubated in 12-well plates for 48 h in a CO_2 incubator (5 % CO_2, 37 °C, humidified atmosphere) in RPMI medium supplemented with OMK derivatives (final concentrations 1 µM, 25 µM, and 50 µM). The OMKs were pre-dissolved in DMSO, with a final concentration of 0.1 % (*v/v*) DMSO in the medium. The negative control consisted of medium with DMSO (0.1 % *v/v*) only, while the positive control comprised 10 µM levamisole in the medium. Following the incubation, the nematodes were collected in sonification solution (SONOP), consisting of 70 % ethanol with 2 mM EDTA (ethylenediaminetetraacetic acid)), frozen immediately in dry ice, and stored at −80 °C. ATP concentration was quantified by the chemiluminescence method according to the manufacturer's protocol (ATP Bioluminescence Assay Kit CLS II, Roche, Mannheim, Germany) and total protein content (µg/mL) was determined by the bicinchoninic acid assay (BCA) method according to the manufacturer's protocol (PierceTM BCA Protein Assay Kit, ThermoScientific) (Zajíčková et al., 2021). When screening measurements of all derivatives were performed, measurements were duplicated. In the case of measurements of selected derivatives, statistics were performed as described in Section 2.21.

2.13. Cultivation of C. elegans

The wild-type *C. elegans* Bristol strain N2 (a kind gift from the Laboratory of Molecular Parasitology, Faculty of Environmental Sciences, Czech University of Life Sciences, Prague, CZ) were cultured at 21 °C on nematode growth medium (NGM) agar plates (1.7 % Bacto agar, 0.2 % Bacto peptone, 51 mM CaCl, 5 mg/l cholesterol, 1 mM $CaCl_2$, 1 mM $MgSO_4$, and 25 mM KPO_4 buffer) seeded with *Escherichia coli* strain OP50 as a food source as previously described (Brenner, 1974). To achieve population synchronization, gravid adults were selected and transferred with a worm picker to the new cultivation plates containing NGM agar seeded with *E. coli*. After 89 h, the population comprising most eggs was collected. All stages except the eggs were lysed with a bleaching mixture (1 volume of 5 M NaOH, sodium hypochlorite 10–15 %, and M9 solution [3 g KH_2PO_4, 5.68 g Na_2HPO_4, 5 g NaCl, and 0.25 g $MgSO_4 \cdot 7\ H_2O$ in 1 l of water]). To remove the toxic bleaching mixture, three washes with M9 solution were conducted. The eggs of *C. elegans* were hatched overnight at 21 °C in M9 solution devoid of bacteria, thereby obtaining a synchronized first-stage larval (L1) population.

2.14. Larval development assay in C. elegans

Approximately 25 L1 larvae were added to each well of a 96-well plate containing S-Basal (5.85 g NaCl, 1 g K_2HPO_4, and 6 g KH_2PO_4 in 1 l of water) completed with 10 ml of 1 M potassium citrate, 10 ml of trace metal solutions, 3 ml of 1 M $CaCl_2$, 3 ml of 1 M $MgSO_4$, 1 ml of cholesterol (5 mg/ml in ethanol) in 1 L of S-Basal and concentrated *E. coli* (1 mg/ml) at the final volume of 200 µl/well. To each well, 1 µl of OMK207 or OMK211 (pre-dissolved in DMSO) to reach 1 µM, 25 µM, 50 µM final concentrations or 1 µl of pure DMSO (as a control) was added in three technician replicates. The plate was incubated at 21 °C for 74 h, during which time the control group of L1 larvae underwent complete development into adult worms. The L1, L2, and L3 larvae were evaluated as being inhibited in their development, while the late L4 and young adult worms were classified as being developed.

2.15. In vitro cytotoxicity and mitotoxicity assays

The potential hepatotoxicity of all derivatives was evaluated using precision-cut liver slices (PCLS) prepared from the liver of sheep. After the sacrifice of the sheep, one lobe of the liver was excised, perfused with chilled Euro Collins solution, and transported to the laboratory in a chilled vessel. The PCLS preparation was previously described in detail (Zárybnický et al., 2018). Freshly prepared PCLS were incubated in Williams' E medium with OMKs (in final concentrations of 1 µM, 25 µM, 50 µM) for 24 h in a CO_2 incubator (5 % CO_2, 37 °C; humidified atmosphere). All derivatives were pre-dissolved in DMSO (to gain final DMSO concentration of 0.1 %, *v/v*). The negative control comprised medium with DMSO (0.1 %, *v/v*), while the positive control contained 10 µM acetaminophen (APAP). after the incubation period, the PCLS were washed with PBS, placed in SONOP solution, frozen in dry ice, and stored in a freezer (−80 °C). An ATP-based method was employed to assess viability, as detailed in (Nguyen et al., 2021).

The human epithelial colorectal adenocarcinoma Caco-2 cell line (ATCC, supplier for the Czech Republic: LGC Standards, Poland) was also used. This cell line was cultured in EMEM supplemented with 10 % (*v/v*) heat-inactivated fetal bovine serum, 1 % (*v/v*) non-essential amino acids, 1 % (*v/v*) glutamine, and 0.5 % penicillin/streptomycin. The cells were cultivated for 21 days in a humidified atmosphere containing 5 % CO_2 at 37 °C. The medium was changed twice a week. The OMK207 and OMK211 were initially dissolved in DMSO. The concentration of DMSO in the medium was 0.1 %. The cells were cultured in 96-well plates and treated with various concentrations (0–50 µM) of OMKs for 72 h. The cells cultured in medium with 0.1 % DMSO were used as a negative control, while cells exposed to 10 % DMSO served as a positive control. Immediately after incubation, the viability was measured by adding

WST-1 (4-[3-(4-Iodophenyl)-2-(4-nitro-phenyl)-2H-5-tetrazolio]-1,3-benzene sulfonate). After 1 h of incubation, when the viable cells converted yellow, water-soluble WST-1 to a purple water-insoluble formazan, the cells and formazan crystals were dissolved by replacing of culture medium with isopropanol containing 0.08 M of hydrochloric acid (HCl) and incubated for 30 min (37 °C, 600 rpm, Thermomixer Comfort, Eppendorf). Subsequently, the absorbance was measured at 570 nm, with a background subtraction at 690 nm (Spark Control Tecan, v. 2.2).

The cytotoxic and mitotoxic activity of OMK207 and OMK211 on HepG2 human hepatoma cells was also evaluated using an established protocol (Kamalian et al., 2015; Sliwka et al., 2016). The test compounds were serially diluted (7-points, 2-fold serial dilution, 1.56–100 μM) in Dulbecco's modified Eagle medium (DMEM) with GlutaMax™ supplemented with 25 mM D-glucose (cytotoxicity) or D-galactose (mitotoxicity), 10 % heat-inactivated foetal bovine serum (FBS), 100 IU/ml of penicillin, 100 μg/ml of streptomycin and 0.25 μg/ml of amphotericin B (designated DMEM*). Monepantel and moxidectin (prepared in the same manner as the test compound) were included as reference compounds. Two compounds, doxorubicin (cytotoxic; Sigma-Aldrich, USA) and M-666 (mitotoxic (Le et al., 2018);), were used as positive controls at a single concentration of 10 μM. A solution of DMEM* +0.25 % (*v/v*) DMSO was used as a negative control. HepG2 cells were seeded into wells of a 96-well plate in 80 μl of DMEM* (at 1 × 10^5 cells per well) and allowed to adhere for 16 h at 37 °C and 5 % (*v/v*) CO_2 at > 90 % humidity prior to incubation with individual compounds, at a final volume of 100 μl. For the assessment of mitochondrial toxicity, cells were starved of serum (DMEM* without FBS) for 4 h prior to the incubation with compounds (Swiss et al., 2013; Kamalian et al., 2015) for the metabolic switch. Following 48 h of incubation with compounds, cell viability was determined by crystal violet staining (Sliwka et al., 2016). The absorbance (595 nm) of treated cells was normalized using the negative controls (viability: 100 %) to calculate the cell viability. All compounds and controls were tested in triplicate. To determine the half-maximal cytotoxic concentration (CC_{50}) and half-maximal mitotoxic concentration (MC_{50}) values, compound concentrations were log_{10}-transformed, baseline-corrected using a respective positive control (doxorubicin or M-666) and fitted using a variable-slope four-parameter equation and ordinary least squares fit model using GraphPad Prism (v.10.3.1).

2.16. *In vivo toxicity testing in mice*

An *in vivo* acute oral toxicity test was conducted in accordance with the OECD test guideline No 425. A total of five adult male mice (ICR strain, Velaz, s.r.o., Czech Republic) were used for each compound (OMK207 and OMK211). Prior to administration, the mice were fasted for 6 h. A single dose of 2000 mg/kg bw in a suspension of methylcellulose (0.5 % in H_2O) was administered to each mouse via oral gavage under general anaesthesia (isoflurane) with a 38 mm plastic gavage tube (Instech Laboratories, Plymouth Meeting, PA, USA). Food was returned 1 h after the substance administration. The mice were observed (mice behaviour, body weight, food and water intake, urine and faeces production, coat, skin and tail condition) for the following 14 days. Subsequently, the mice were sacrificed and dissected for organ condition evaluation.

2.17. *Target identification using thermal proteomic profiling (TPP)*

Thermal proteome profiling (TPP) is an advanced, multiplexed mass-spectrometry method for the identification of drug targets. It relies on the thermostability of protein-drug interactions through denaturation profiles (melting curves) upon heat treatment. The present study followed an established TPP protocol (Savitski et al., 2014), comprising five steps (i.e., preparation of parasite protein extracts; incubation with compound and "heating" of samples; protein digestion and peptide labelling; mass spectrometric analysis; and data processing) as described in (Taki et al., 2022) with mild modification.

2.17.1. *Preparation of protein extracts from H. contortus*

approximately 70 adults (mix of males and females) were frozen in liquid nitrogen and ground to a fine powder using a mortar and pestle, transferred to a 2-ml homogenization tube, suspended in 1.5 ml ice-cold phosphate-buffered saline (PBS, pH 7.0) containing 0.5 % (*v/v*) nonylphenoxypolyethoxylethanol (NP-40), homogenized using Potter-Elvehjem system and centrifuged at 20,000×*g* for 20 min at 4 °C. Subsequently, the supernatant was collected and the protein (measured using a BCA Protein Assay Kit, Thermo Fisher Scientific) was adjusted to 2 mg/ml and divided into four 250 μl protein extract aliquots.

2.17.2. *Incubation with OMK211, and temperature profile*

Two test samples with protein extract were each incubated with 250 μl of PBS (pH 7.0) containing OMK211 (final concentration 20 μM, predissolved in DMSO) and two control-samples with an equal volume of PBS with DMSO only for 30 min at 23 °C. Each of the samples was partitioned into 10 PCR tubes (49 μl each); individual pairs of test- and control-samples were simultaneously incubated in a thermal cycler (Applied Biosystems) at 10 distinct temperatures (37, 41, 44, 47, 50, 53, 56, 59,63 and 67 °C) for 3 min. Subsequently, all 40 tubes were ultracentrifuged 100,000×*g* for 20 min at 4 °C, and soluble proteins (i.e., from above the pellet) collected into fresh tubes (each containing 45 μl).

2.17.3. *Protein digestion and TMT labelling*

Proteins (10 μg) from each tube were bound to magnetic HILIC beads according to the SP3 protocol (Hughes et al., 2019). After washing out the buffer with 80 % ethanol, the protein-bead mixture was resuspended in 100 mM triethylammonium bicarbonate (TEAB) and the disulfide bridges were reduced with 10 mM Tris(2-carboxyethyl)phosphine (TCEP) and the cysteines were modified with 50 mM chloroacetamide (one step reaction 30 min in 60 °C). Two micrograms of trypsin was added to the reaction and the proteins were digested until the next day at 37 °C. The collected supernatant was acidified with trifluoroacetic acid (TFA) to a final concentration 1 %. Peptides were desalted on a home-made desalting column (Kulak et al., 2014) and reconstituted in 10 μl 100 mM TEAB. Then, 4 μl of TMT 10-plex label (0.8 mg resuspended in 42 μl of anhydrous acetonitrile) was added to each sample. The samples were incubated for 1 h and the reaction was stopped by the addition of 1.5 μl of 5 % hydroxylamine. After evaporation, the samples were desalted on a Opti-trap cartridge C18 column.

2.17.4. *LC-MS analysis*

The resulting mixture was fractionated on a reverse phase at high pH, flow 2 μl/min, YMC column (300 mm, 0.3 mm, 1.9 mm), linear 60 min gradient (A – 20 mM NH_4FA/2 % ACN; B – 20 mM NH_4FA/80 % ACN) from 1 % B to 60 % B (Kulak et al., 2017). Subsequently, 64 fractions were collected and combined into 8 resulting pooled fractions by the farthest neighbour method (Wang et al., 2011). The fractionated peptides were resuspended in 1 % TFA/2 % ACN and roughly 1.5 μg injected onto nanoHPLC Dionex Ultimate 3000RS in combination with Thermo Orbitrap Ascend. Thermo PepMap Trap column (pn: 160,454) was used for peptides preconcentration and main separation was done on 25 cm Aurora Ultimate Column (Ionoptiks). Each fraction was separated on a 150 min gradient from 2 % A to 35 % B (A - 0.1 % FA, B 99.9 % ACN/0.1 % formic acid). Cycle time was set to 3 s. The MS^2 spectra for identification were measured in an ion trap with CID fragmentation, 60 ms maximum injection time. The real-time search function was used and only identified spectra were submitted to the quantification with MS^3 fragmentation 118 ms maximum injection time, 10 precursors for synchronous precursors selection feature (Le et al., 2020).

2.17.5. *Raw LC-MS data processing*

Raw data from each biological replicate were searched with

Proteome Dicoverer 3.1 with Sequest search engine. The method was based on a predefined workflow for SPS Realtime search MS3 isobaric quantification and was used with batch specific correction parameters for the TMT 10-plex label. Database of *H. contortus* (20953 entries) from UniProt was used for search along with common contaminants. Dynamic modification were set as follows: Oxidation/+15.995 Da (M). Protein N-Terminal: Acetyl/+42.011 Da, Met-loss/−131.040 Da (M), Met-loss + Acetyl/−89.030 Da (M). Static Modifications: Carbamidomethyl/+57.021 Da (C), TMT 6-plex/+229.163 Da (K), Peptide N-Terminus: TMT 6-plex/+229.163 Da. For the assessment of false discovery rate, percolator was used. For reporter ions detection, 20 pmm tolerance was set with the most confident centroid peak integration. Non-normalized and non-scaled abundances for each channel of TMT plex were exported and submitted into the TPP package for the R Bioconductor environment (6). Two controls and two treatments for each tested compound. Proteins with significantly changed melting temperatures were considered as possible interactors.

2.18. Protein structure prediction and protein-ligand docking

The three-dimensional structure of the identified protein was obtained from UniProt database created by the algorithm AlphaFold2 (Jumper et al., 2021). To predict the interaction between the identified protein and the OMK211 compound, the docking server CB-Dock2 (https://cadd.labshare.cn/cb-dock2/) was used for automated cavity detection (Liu et al., 2022). The cavity which is located within one domain only (not across multiple domains) was selected for the blind docking prediction of the OMK211 binding using default settings.

2.19. Phylogenetic analysis

The orthologous proteins were selected using the NCBI BLASTp tool searching for proteins with the same set of domains having above 50 % identity. The amino acid sequences were aligned using Muscle algorithm in MEGA software (Tamura et al., 2021). Phylogenetic relationship was inferred using Maximum Likelihood method with "JTT + G" as the best-fitting model for phylogenetic comparison (Jones et al., 1992). Initial tree(s) for the heuristic search were obtained by applying the Neighbour-Joining method to a matrix of pairwise distances estimated using a JTT model. A discrete Gamma distribution was used to model evolutionary rate differences among sites (4 categories (+G, parameter = 0,4811)). The analysis involved 17 amino acid sequences. All positions with less than 85 % site coverage were eliminated. That is, fewer than 15 % alignment gaps, missing data, and ambiguous bases were allowed at any position. There was a total of 753 positions in the final dataset.

2.20. Transcriptomic analysis

The transcriptomic analysis was performed similarly as described in Štěrbová et al. (2023). Briefly, the RNA was isolated from 100,000 eggs, 100,000 L1, 30,000 L3, 15 adult males or 10 adult females of *H. contortus*, with four biological replicates used per each stage. The RNA was isolated using TriReagent® (Molecular Research Centre, OH, United States) according to the manufacturer's recommendations. The cDNA was synthesized from 0.5 μg of RNA. The relative expression of *Hco*_C2 along with GAPDH as reference gene was analysed by qPCR using SYBR Green I detection, conducted in technical duplicates. The primers were designed using Primer3 software and synthesized by Generi Biotech, Czech Republic. Prior to the qPCR analysis, the specificity and efficiency of the primers were verified.

2.21. Statistical analyses

All data presented in the experiments were analysed using GraphPad Prism 10.1.2. Statistical significance was determined at a p-value of less than 0.05. The EHT was performed in two independent experiments, each with two technical replicates in each. The viability experiments (ATP method) were conducted in four independent experiments, with four biological replicates in each experiment. The results were analysed using a one-way ANOVA with Dunnett's multiple comparison test to evaluate the concentration dependency on viability, and a two-way ANOVA with Šídák's multiple comparison test to compare the strains and gender. Tests of motility were performed in two independent experiments, with three technical replicates. Two-way ANOVA with Tukey's multiple comparisons test was used for the statistical analysis. Hepatotoxicity tests were performed in three independent experiments, with each experiment comprising three technical replicates. One-way ANOVA with Dunnett's multiple comparison was used for the statistical analysis. Tests of *C. elegans* larval development were performed in three technical replicates. For the statistical analysis was used dose-response – inhibition test. The transcriptomic analysis was performed using four biological replicates and qPCR was run in duplicates. All results are presented as mean ± SD.

3. Results

3.1. Synthesis of OMK derivatives

To improve the anthelmintic activity of the benzhydroxamic acid derivative BLK127 we synthesized a mini-library of 13 novel analogues (Fig. 1). For this purpose, we modified the 4-pentyloxy substituent (pentylether moiety) and the benzyloxyamide motif of BLK127 using a bioisosteric approach. For the synthesis of the novel BLK127 analogues (OMK198-OMK212), 4-butoxy-, 4-pentoxy-, and 4-hexoxy benzoic acid (1a-c) were reacted with differently substituted O-substituted hydroxylamine hydrochlorides (2a-k) in the presence of HATU/DIPEA.

3.2. Physico-chemical properties of OMKs

The chemical stability of OMKs in an aqueous solution (phosphate buffer, pH 7.4) was determined to guarantee chemical stability during *in vitro* and *in vivo* studies. Results of OMK211 testing is presented in Table 1. After 48 h no decomposition of OMK211 was detected by HPLC analysis.

3.3. Inhibition of eggs hatching in H. contortus

First, the effect of all OMK derivatives (concentration range 0.5–50 μM) and positive control thiabendazole on egg hatching was evaluated using the *H. contortus* ISE strain. From the entire collection of 13 OMKs, only OMK207 demonstrated a statistically significant inhibitory effect on egg hatching (data not shown). Subsequently, the inhibitory potential of OMK207 was tested in eggs of the ISE and WR strains. In both

Table 1
The results of testing of chemical stability of OMK211.

	date/time	Retent. Time [min]	Area [Au.s]	Height [AU]	Area [%]	Height [%]
Start 0h	November 05, 2024 08:48	14.504	5.924	0.862	100	100
1 h	November 05, 2024 09:49	14.496	5.927	0.867	100	100
3 h	November 05, 2024 11:49	14.479	5.993	0.863	100	100
6 h	November 05, 2024 08:48	14.488	6.008	0.845	100	100
24 h	November 06, 2024 08:48	14.497	5.975	0.866	100	100
48 h	November 07, 2024 08:49	14.491	6.043	0.847	100	100
	Mean	14.493	5.978	0.858	100	100
	S.D.	0.009	0.047	0.010	0.000	0.000

H. contortus strains, OMK207 significantly reduced the number of hatched eggs with an IC_{50} 28.5 ± 2.71 and 30.69 ± 4.15 μM in the ISE and WR strains, respectively (see Fig. 2).

3.4. Inhibition of H. contortus xL3 motility and development

The effect of all OMK derivatives (concentration range: 0.4–100 μM) on xL3s was evaluated using the *H. contortus* Haecon-5 strain. From the panel of 13 OMKs, OMKs 207 and 211 demonstrated a statistically significant inhibitory effect on larval motility and development. OMKs 207 and 211 exhibited most potency *in vitro*, being almost equipotent for motility (IC_{50} = 19.6 ± 2.37 and 21.1 ± 3.77 μM) and development (IC_{50} = 14.2 ± 0.02 and 17.3 ± 0.50 μM) inhibitions (see Fig. 3). OMK206 also induced moderate motility and development inhibitions (IC_{50} values of 52.7 ± 6.74 and 41.3 ± 3.21 μM, respectively).

3.5. Effect of OMK derivates on H. contortus adults

The effect of all OMK derivatives (at concentrations 1, 25, and 50 μM) and the positive control levamisole (10 μM) on nematode viability (as measured by ATP concentration normalized with respect to protein content) was initially screened separately in adult males and females of the ISE strain of *H. contortus*. Due to screening measurements, there was insufficient replication for statistical analysis. Of all 13 OMKs, OMK207 and OMK211 had the strongest effect on the viability of *H. contortus* adults, with a more pronounced effect observed in males compared to females (Fig. 4).

Consequently, the activities of OMK207 and OMK211 were separately evaluated and compared in adults of the ISE and WR strains. The results are presented in Figs. 5 and 6. In the adults of *H. contortus* ISE strain, a notable decline in viability was observed at the lowest concentration of both OMK derivatives, with more pronounced efficacy in males than in females. In the WR strain, OMK207 was active in males at the lowest concentration tested (1 μM), exhibiting an inhibitory effect comparable to that of levamisole (10 μM). However, the effect of OMK207 on the viability of females of the WR strain was not statistically significant. In contrary, OMK211 significantly reduced the viability of both females and males of the WR strain of *H. contortus*.

Subsequently, the effects of OMK207 and OMK211 on the motility of *H. contortus* females of the Haecon-5 strain was tested. The results (Fig. 7) showed that OMK211 is a potent inhibitor of *H. contortus* motility, exhibiting the degree of efficacy that is comparable with the positive control monepantel. Both OMK211 and monepantel inhibited the motility completely (100 % inhibition) by 24 h. In contrast, OMK207 had no significant effect on adult motility.

3.6. The effect of OMK207 and OMK211 C. elegans development

A synchronized L1 population of *C. elegans* was exposed to varying doses of OMK207 and OMK211, followed by 74 h of growth at 21 °C in S-Basal medium. The development was calculated as a percentage of adults in the presence of the tested compounds normalized to the untreated control. OMK207 and OMK211 inhibited the development of *C. elegans* with IC_{50} 13.63 ± 0.72 and 23.26 ± 0.72 μM, respectively (see Fig. 8)

3.7. The effect of OMK207 and OMK211 derivatives on viability of PCLS and differentiated Caco2 cells

The potential toxicity of OMK207 and OMK211 (at concentrations of 1; 25 and 50 μM) was evaluated *in vitro* using ovine precision-cut liver slices (PCLS) and enterocyte-like differentiated Caco2 cells. The viability of liver cells was not adversely affected by any of the tested compounds, in contrast to the positive control, 10 μM APAP, which resulted in a 60 % reduction in PCLS viability. Similarly, the tested compounds were not toxic in differentiated Caco2 cells, whereas 10 % DMSO was lethal to all cells (see Suppl. 2).

3.8. The effect of OMK207 and OMK211 derivatives on HepG2 cells

The potential cytotoxicity and mitotoxicity of OMK207 and OMK211 (concentration range 1.56–100 μM) was evaluated *in vitro* using HepG2 human hepatoma cells. Neither derivative exhibited no cytotoxic (CC_{50} > 50 μM) or mitotoxic (CC_{50} > 50 μM) effects on HepG2 cells, in contrast to the positive controls, doxorubicin (cytotoxic) or M-666 (mitotoxic), which resulted in a 100 % toxicity at 10 μM. However, OMK211 at a concentration of 100 μM was cytotoxic in HepG2 cells (Fig. 9).

3.9. The effect of OMK207 and OMK211 in mice in vivo

The compounds OMK207 and OMK211 (administered in a single dose of 2000 mg/kg bw) were administered to five mice by oral gavage. No mortality was observed in the mice during the 14-day post-administration period. In the group treated with OMK207, a negative effect on the mice's behaviour (apathy and tremors) was observed up to 48 h post-administration. Additionally, OMK207 decreased food consumption and the production of urine and faeces during the initial 24-h period. The mean decrease in body weight for the OMK207-treated animals was 7 %, though this returned to the initial body weight within the subsequent 24 h. Two animals exhibited evidence of tail tip necrosis 48 h post-administration. In the group treated with OMK211, no adverse effects were observed in mice and the compound was well tolerated. The dissection of mice 14 days after administration revealed

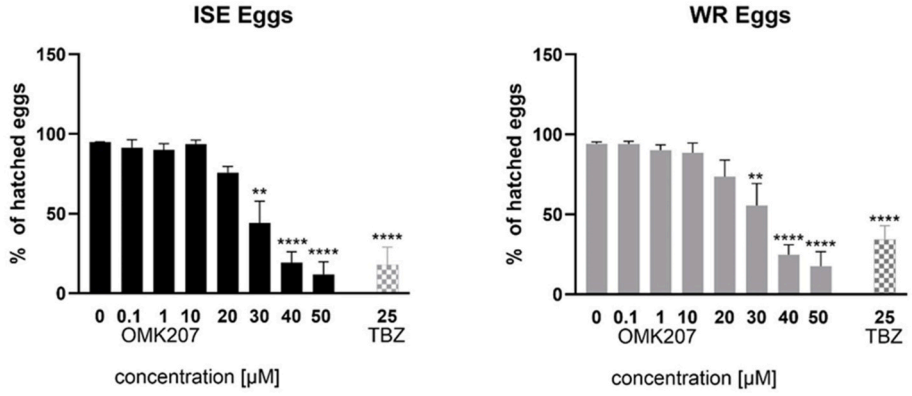


Fig. 2. The effect of derivates OMK207 (at concentration range 0–50 μM) and TBZ (25 μM) on H. contortus eggs of the ISE and WR strain after 48 h incubations. The data are expressed as percentage (%) of eggs hatched (±SD). *Indicates a significant difference between the untreated (negative control) and treated eggs within the strain at $P < 0.05$.

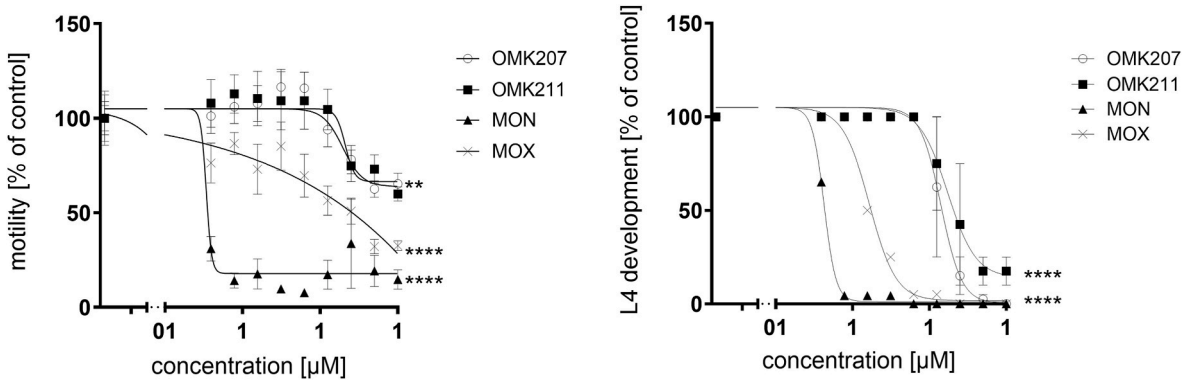


Fig. 3. The effect of derivates OMK207 and OMK211, monepantel (MON) and moxidectin (MOX) on *H. contortus* xL3s of the Haecon-5 strain after 90 h (motility) and 168 h (development) incubations. The data are expressed as % of motile or developed larvae ± SD. *Indicates a significant difference between the lowest (0 µM) and highest (100 µM) concentrations within the compounds at **P ≤ 0.01 and ****P ≤ 0.0001.

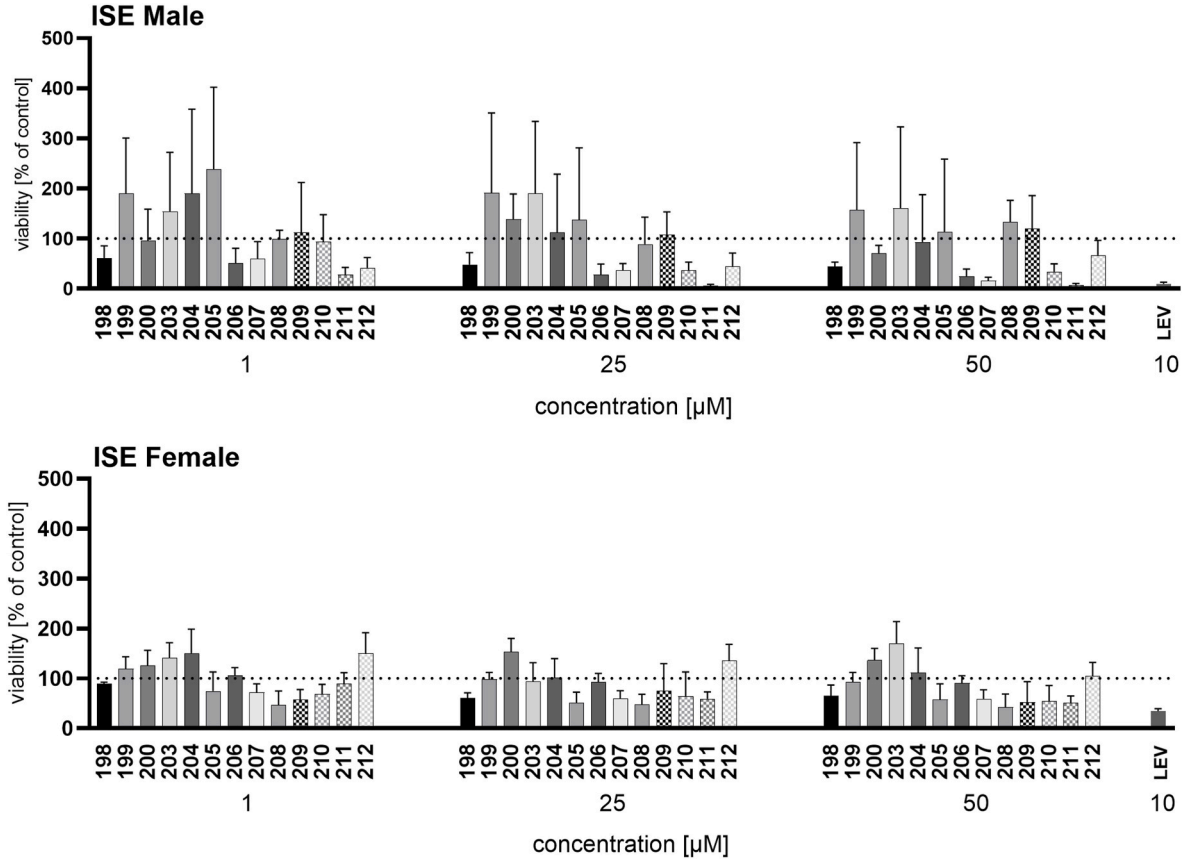


Fig. 4. The screening of the effect of OMKs (198–212) derivatives (at concentrations 1, 25 and 50 µM) and levamisole (LEV; 10 µM) on the adults of *H. contortus* ISE strain. The data are expressed in percentage of viability of the untreated controls (=100 %) ± SD.

no observable adverse effects on tissues and organs associated with either compound.

3.10. Investigation of OMK211 target in H. contortus adults

Based on the promising activity of OMK211, we aimed to search for the putative target of this compound. We employed thermal proteome profiling (TPP) and overall identified 5557 proteins in homogenate from *H. contortus* adults. Altogether 2256 proteins were detected in all samples analysed (see Fig. 10A); OMK211 treated, and control samples run in duplicates. Relative protein abundance decreased with temperature (see Fig. 10B). Following filtering we identified one protein (encoded by gen HCON_00184,900) which exhibited higher statistically significant thermostability in the presence of OMK211 with refence to the DMSO control (Fig. 10C). The shift in thermostability suggests this protein may be an OMK211 target.

The identified possible target is a C2-domain containing protein (A0A6F7Q0A8, HCON_00184,900), which we named *Hco*_C2 protein. The *in silico* analysis showed several domains present within the sequence (820 aa); a C2 domain (IPR000008) which is predicted as calcium-dependent phospholipid binding or/and in membrane targeting processes such as subcellular localization. Another well recognized domain within this protein is a protein kinase C1 domain or a phorbol-ester/diacylglycerol-binding domain (IPR002219), which presumably

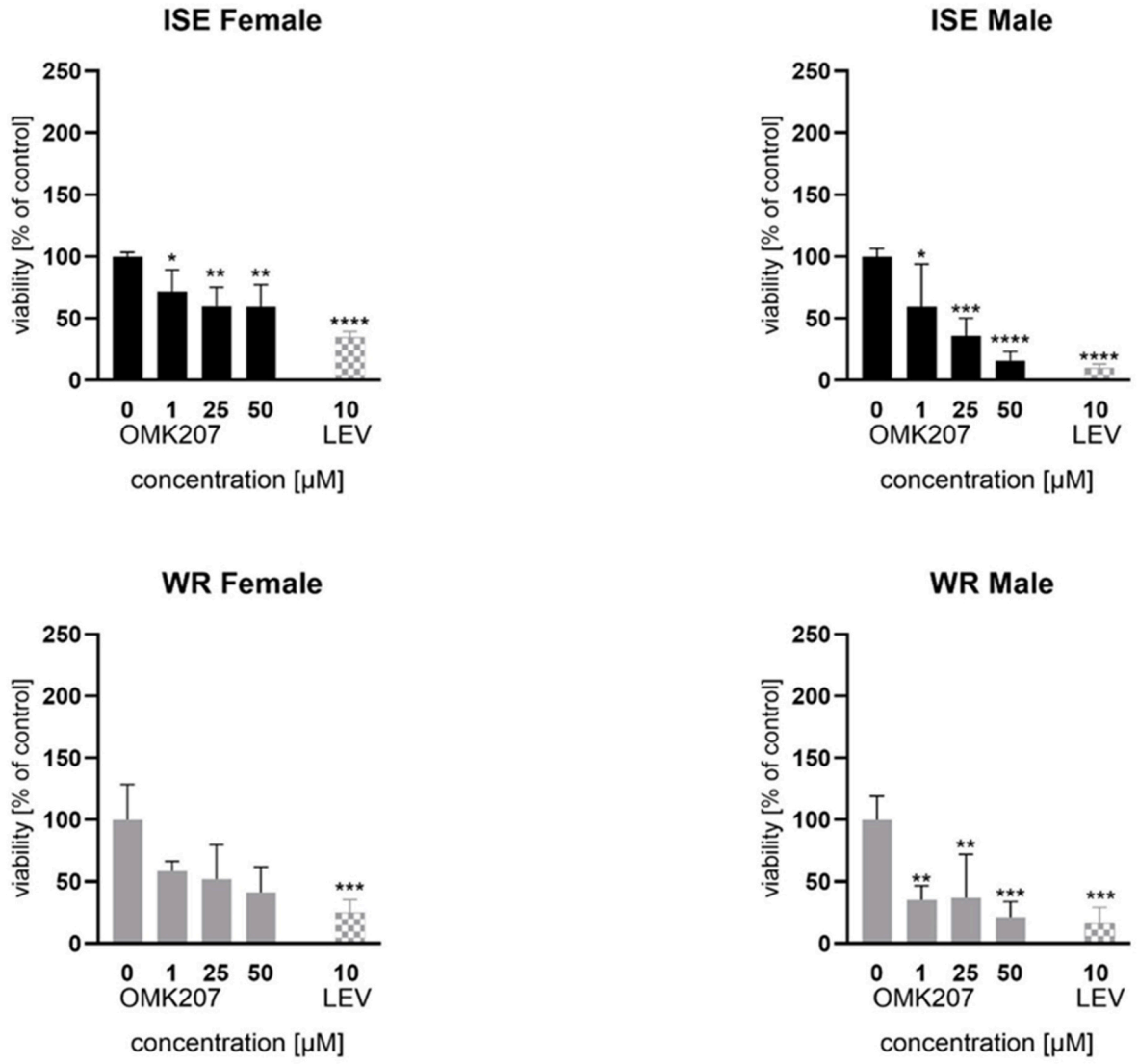


Fig. 5. The effect of OMK 207 on viability of *H. contortus* adults (male and female) of the ISE and WR strains after 48 h incubations. The data are expressed in percentage of viability of the controls (=100 %) ± SD. The asterisks indicate a significant difference between the control and inhibitor groups within the strain (ISE) at: *, $P < 0.05$; **, $P < 0.01$; ***, $P < 0.001$; ****, $P < 0.0001$.

binds two zinc ions, however, function of which is unknown. The AlphaFold2 has predicted third well packed domain, all of them with variable confidence level as can be seen by different pLDDT (see Fig. 11A). We employed the CB-Dock tool to predict potential binding of OMK211. There were five potential binding sites (cavities) predicted, Fig. 11B shows the binding prediction with the best Vina Score (−7.9), the potential contact residues are all located with the uncharacterized domain located close to the N-terminus of the protein.

The BLAST search against the *H. contortus* genome (Project PRJEB506) revealed only two transcripts from the same gene resulting in unique protein sequence. The BLAST results from WormBase against *C. elegans* genome (project PRJNA13758), revealed four isoforms of protein R11G1.6(a-d), gene designated *tmem-24*. The pairwise comparison showed only 60.4 % identity of the overlapping region (the translated protein in WormBase has 90 amino acids long extension on the N-terminus, however, the respective protein in UniProt database – Q7Z1P8 does not have this extension). Transcriptomic analysis shows the HCON_0018,490 gene expression in all developmental stages of *H. contortus*, with expression level in males being tenfold higher than in females (see Fig. 12A).

The BLASTp results in the NCBI protein database revealed 16 sequences from various nematodes having above 50 % identity. Phylogenetic analysis of the *Hco*_C2 protein with its orthologs in sixteen other nematode species shows classical clustering (Fig. 12B). Less similar (<50 % identity) were unknown proteins containing the same set of identified domains from the phylum Insecta or Eleutherozoa. The BLASTp (NCBI) search across mammalianproteomes showed that only the PE/DAG-binding domain is somewhat similar. When only the domain near the N-terminus of unknown function (amino acids 40–240) containing the predicted OMK binding pocket were used for the BLAST search no significant similarity in mammals was found.

4. Discussion

Here, we synthesized and evaluated 13 novel derivatives of benzhydroxamic acid (OMKs) for their nematocidal or nematostatic effect on different developmental stages of *H. contortus*. This parasitic nematode was selected because it represents a socioeconomically significant, pathogenic nematode with a high reproductive index that can be readily maintained in a laboratory environment and because it is relatively closely related to the free-living nematode *Caenorhabditis elegans* (within evolutionary clade V) – one of the best studied and understood

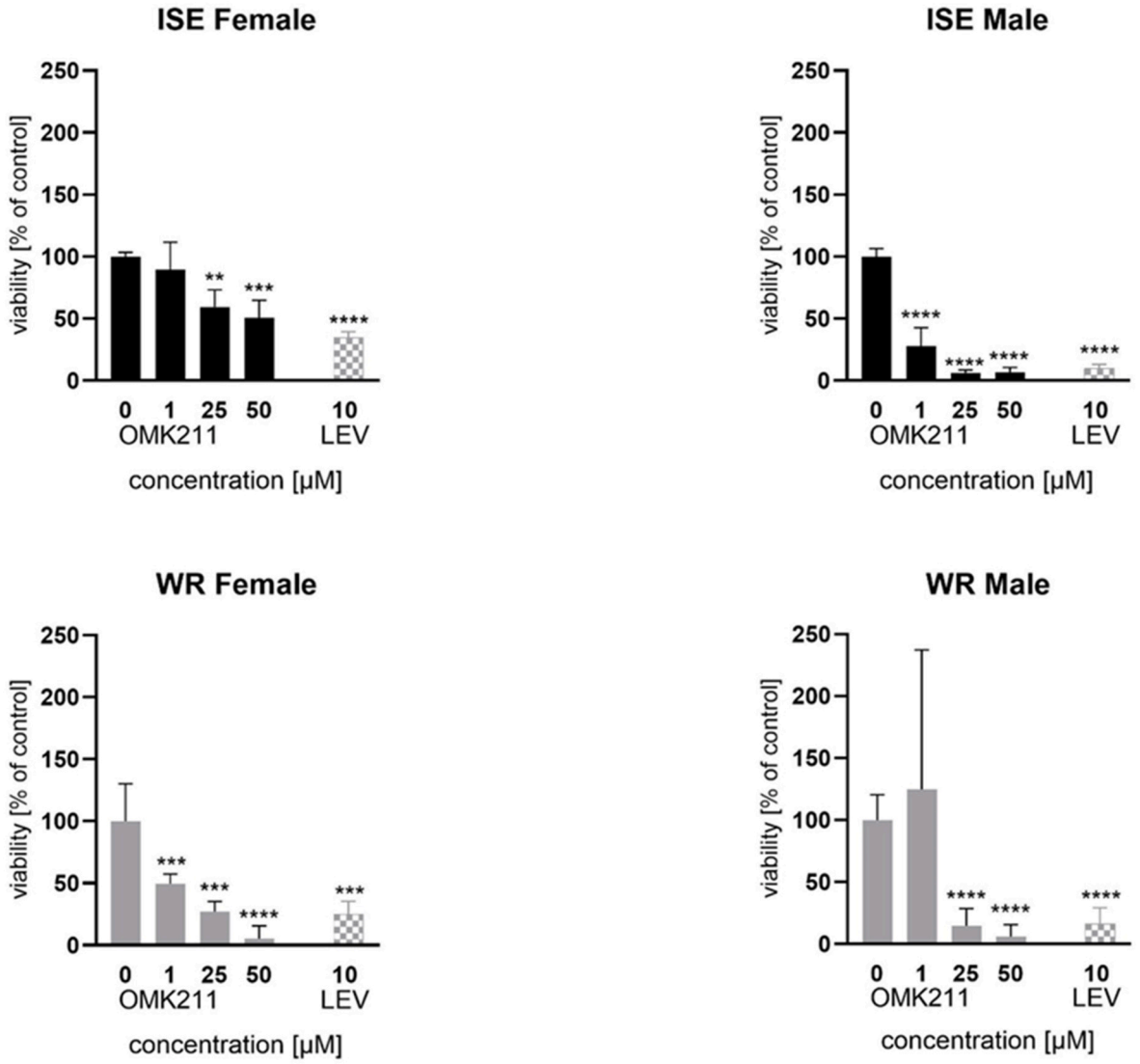


Fig. 6. The effect of OMK 211 on viability of *H. contortus* adults (male and female) of the ISE and WR strains after 48 h incubations. The data are expressed in percentage of viability of the controls (=100 %) ± SD. The asterisks indicate a significant difference between the control and inhibitor groups within the strain (ISE) at: *, P < 0.05; **, P < 0.01; ***, P < 0.001; ****, P < 0.0001.

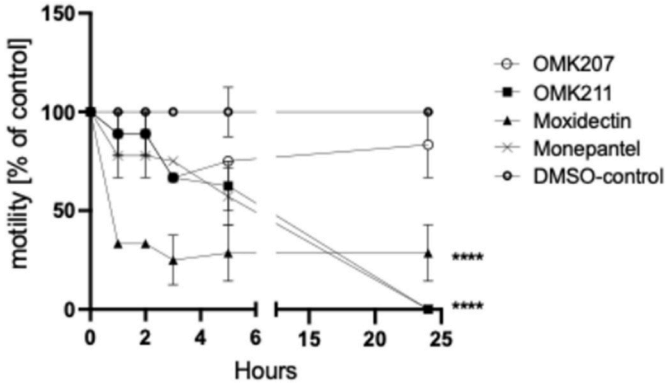


Fig. 7. The effect of OMK207 and OMK 211 on motility of H. contortus adults of the Haecon-5 strain over 24 h incubation. The data are expressed in percentage of motility of the controls (=100 %) ± SD. *Indicates a significant difference between the lowest (0 μM) and highest (100 μM) concentrations within the compounds at ****P ≤ 0.0001.

multicellular organisms (Harris et al., 2019; Davis et al., 2022).

The chemical synthesis process was short, efficient and produced OMK analogues of high purity. The starting materials and intermediates used were readily accessible. After screening OMKs on eggs, xL3 larvae, and adults of the *H. contortus* ISE strain. In the egg hatch test, only OMK207 demonstrated an ovicidal effect, whereas the other derivatives were inactive. Also, the prime benzhydroxamic acid derivative BLK127 did not inhibit egg hatching (Zajíčková et al., 2022). In *H. contortus* larvae and adults, OMK207 and OMK211 demonstrated the most pronounced inhibitory effects on development, xL3 motility and the viability of adults. Based on these results, OMK207 and OMK211 were selected as the most promising candidates for further investigation.

The ovicidal effect of OMK207 was tested and compared in a drug-sensitive strain ISE and in a drug-resistant strain WR. The results demonstrated that the effect of OMK207 was less pronounced than that of the positive control thiabendazole. However, in contrast to thiabendazole, OMK207 exhibited an inhibitory effect on egg hatching to a similar extent in both strains. This finding indicates the OMK target is distinct from that of thiabendazole. Furthermore, it is important to emphasise, that the inhibitory effect on egg development is a distinctive advantage of OMK207, which is not observed in many currently

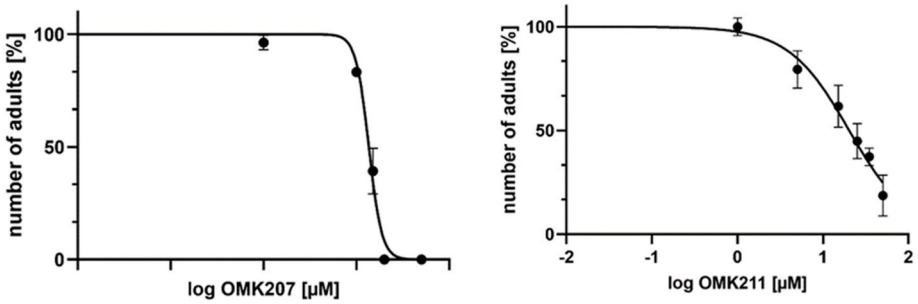


Fig. 8. Effect of OMK207 and OMK211 on the development of *C. elegans* from L1 do adults. The results are shown as a mean with standard deviation and indicate % of developed adult worms compared to the control (incubated with 0.1 % DMSO only) ± SD.

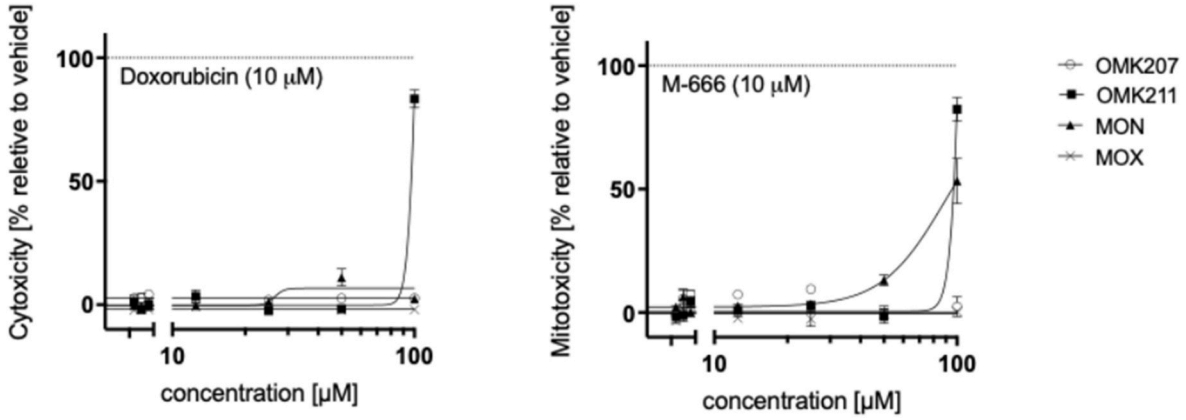


Fig. 9. The effect of derivates OMK207 and OMK211, monepantel (MON) and moxidectin (MOX) on HepG2 cells after 48-h incubations. The data are expressed as % of cyto- or mitotoxicity relative to negative controls (vehicle) ± SD. The maximal toxicity level (100 %) was determined by control compounds, doxorubicin (cytotoxic) and M-666 (mitotoxic; Le et al., 2018) at 10 μM.

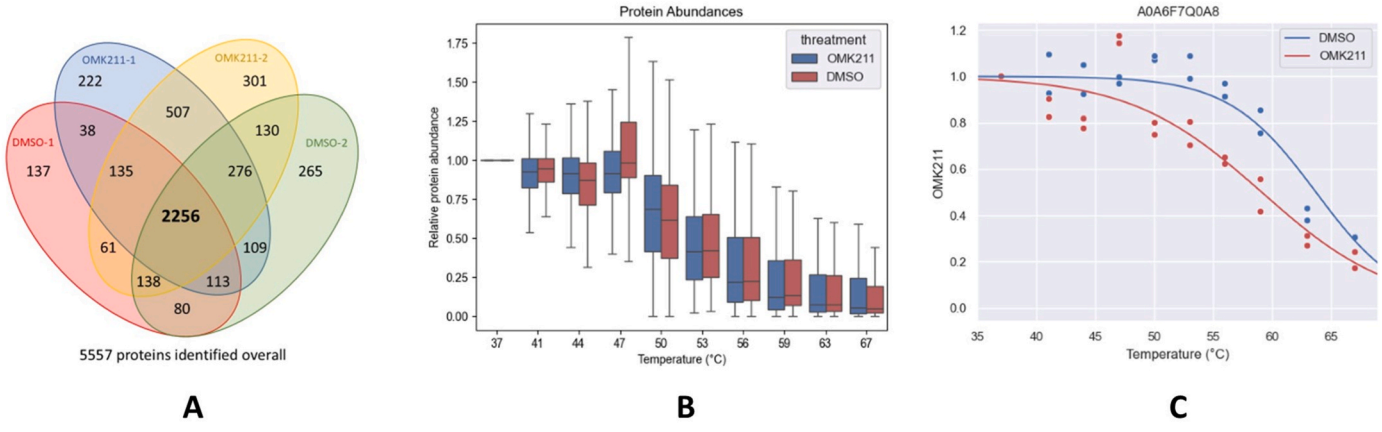


Fig. 10. Thermal proteome profiling (TPP). (A) Venn diagram showing the overall numbers of identified proteins in each sample. (B) Boxplot of overall quantified soluble proteins showing relative fold-change in abundance upon treatment with OMK211 or DMSO in a temperature gradient from 37 °C to 67 °C. (C) Thermal shift plot showing the melting curves of the potential target for OMK: A0A6F7Q0A8 (HCON_00184,900), named *Hco*_C2 protein. Data from two replicates.

available anthelmintics, which can offer an advantage in preventing or limiting the transmission and spread of infection by eggs. Both OMK207 and OMK211 demonstrated a larvicidal effect in *H. contortus* larvae. This effect was also observed in *C. elegans* larvae, with OMK207 being more effective than OMK211. On the other hand, OMK211 exhibited superior anthelmintic efficacy than OMK207 in *H. contortus* adults. In males, OMK211 significantly decreased viability to 25 %, even at a concentration of 1 μM. In comparison to BLK127 (with IC_{50} around 20 μM), OMK211 was much more effective (Zajíčková et al., 2022). These results are particularly important as adults represent the developmental stage of nematodes that need to be targeted by anthelmintic drugs. Moreover, pronounced anthelmintic activity of OMK211 was observed also in adults of the multi-resistant WR strain, with males being more sensitive than females.

As a prospective anthelmintic agent must be toxic to parasitic helminths but not their host(s), the toxicity of OMK207 and OMK211 was evaluated *in vitro* using liver cells (given the liver's sensitivity to xenobiotics) and Caco2 cells – derived from human epithelial colorectal adenocarcinoma, capable of differentiating into enterocyte-like cells (Tran et al., 2002), thus being a suitable model for assessing the

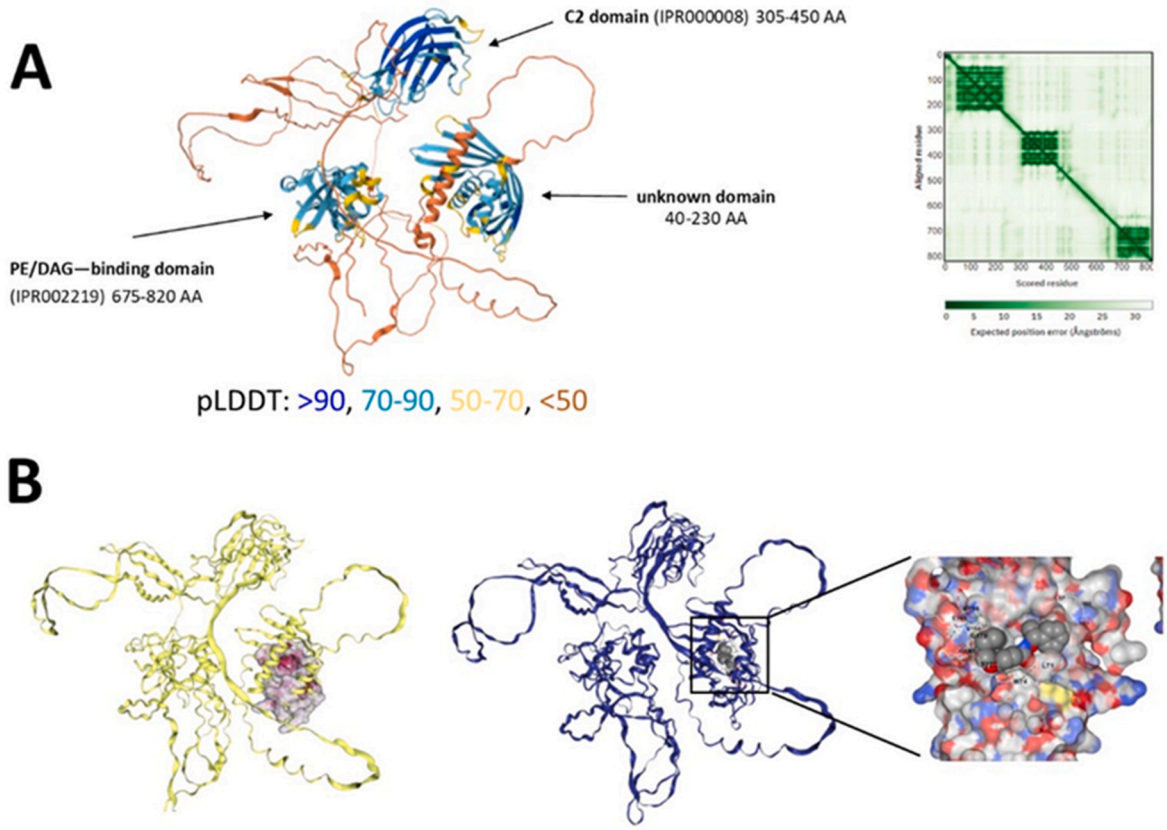


Fig. 11. Predicted structure of *Hco*_C2 protein and docking with OMK. (A) Structure of *Hco*_C2 protein predicted *in silico* using the Alphafold2 algorithm (left). The per-residue confidence scores (pLDDT) are color-coded below the structure. The predicted aligned error (PAE, right) shows three well separated domains. (B) The cavity identification in the three-dimensional structure of *Hco*_C2 protein by CB-Dock (left) and the predicted binding of OMK211 inside this cavity within the unknown domain.

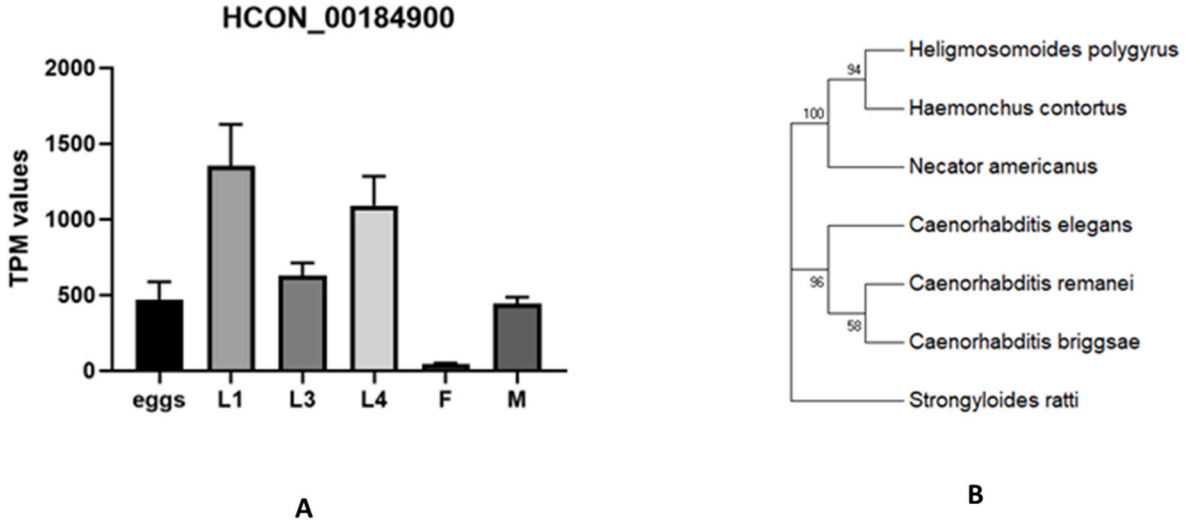


Fig. 12. Expression of *Hco*_C2 and phylogenetic relationship of its orthologs. (A) Relative transcription of *Hco*_C2 in eggs, larvae (L1, L3), adult female (F) and male (M). (B) Phylogenetic relationship of *Hco*_C2 protein (highlighted by black dot) and its orthologs from other nematodes (*Caenorhabditis* abbreviated to C.). The tree with the highest log likelihood (−9159,4077) is shown. The percentage of trees in which the associated taxa clustered together is shown next to the branches. The tree is drawn to scale, with branch lengths measured in the number of substitutions per site.

intestinal toxicity of potential orally administered drugs. Neither compound exhibited any *in vitro* toxicity in mammalian cells up to 50 μM concentration, while they were effective against nematodes from a concentration 1 μM, which indicates their selective toxicity in nematodes. Consequently, *in vivo* toxicity of OMK207 and OMK211 was evaluated in mice. An acute oral toxicity test (OECD test guideline no. 425) was conducted on five mice for each compound. The exceedingly high dose (2000 mg/kg of body weight) of both OMK207 and OMK211 was not lethal to any mouse. While OMK207 exhibited some adverse effects on mice during the initial two-day period following

administration, OMK211 was well tolerated, with no discernible negative impact on the mice.

Based on these findings, OMK211 was identified as a hit compound, and its putative molecular targets in *H. contortus* adults were investigated using thermal proteome profiling analysis (TPP). Published evidence (Savitski et al., 2014; Perrin et al., 2020; Mateus et al., 2022) demonstrates clearly the capacity of TPP in defining target molecules in biomedical projects such as cancer research. In addition, TPP has been employed previously to identify molecular targets of potential anthelmintics using *H. contortus* larvae (Taki et al., 2022). Our TPP analysis revealed C2-domain containing protein A0A6F7Q0A8 (named *Hco*_C2 protein) as a possible interacting partner of OMK211. This orphan protein, encoded by the gene HCON_00184,900, consists of three well packed domains. Using CB-Dock five potential binding sites for OMK211 were predicted. The prediction with the most favourable Vina score (−7.9) is located within the uncharacterized domain near the N-terminus of the protein. The reliability of this predicted binding is supported by the fact that the interacting amino acids are to a single predicted domain. The limited confidence around structure predictions has to be highlighted and therefore further studies are needed.

The BLAST results from WormBase against the *C. elegans* genome, revealed the orthologs, four isoforms of protein R11G1.6(a-d), gene designated *tmem-24*. The pairwise comparison showed only 60.4 % identity in the overlapping region. There is no functional analysis of this protein available, however, the RNAi screen did not reveal any phenotypic change upon silencing of this gene (Kamath et al., 2003). The single cell expression analysis from *C. elegans* reported that *tmem-4* is expressed mainly in pharyngeal muscle cells (Packer et al., 2019). The transcription levels of respective *Hco*_C2 gene showed the highest expression in L1 larvae, followed by L3, eggs and males, which corresponds to data retrieved from the available differential transcriptome sequencing project (PRJEB1360, accession ERP00217R (Laing et al., 2013), based on TPMs (transcripts per million). Significantly higher expression of *Hco*_C2 in adult males than in females corroborates the finding that the anthelmintic effect of OMK211 is higher on males than females. The BLAST results revealed *Hco*_C2 orthologs having above 50 % identity in various nematodes, which indicate the possibility of general nematocidal activity of OMK211. On the other hand, no significant similarity was found in mammals, when the domain with the predicted OMK211 binding pocket was used for the BLAST search. This is quite promising *in silico* result for a potential drug target which support the importance of further exploring the function and binding capacity of this protein in order to employ structural activity relationship analysis of novel OMK analogues. Additionally, the importance of this protein in nematodes should be verified using knock down expression in *C. elegans*.

5. Conclusions

Novel derivatives of benzhydroxamic acid represent a promising new class of anthelmintics. OMK211 can be considered a lead compound with promising nematocidal activity and no detectable toxicity in mammalian cells *in vitro* and in mice *in vivo*. The putative interacting molecule, the *Hco*_C2 protein, may represent an attractive molecular target, as its orthologs are predicted to be present in several nematodes but not in mammals. Following the verification of this target, molecular docking will facilitate further structural optimisation of potential drugs.

CRediT authorship contribution statement

Josef Krátký: Writing – original draft, Methodology, Investigation, Data curation. **Markéta Zajíčková:** Investigation, Data curation. **Aya C. Taki:** Writing – original draft, Methodology, Investigation, Data curation. **Oliver Michel:** Methodology, Investigation, Data curation. **Petra Matoušková:** Validation, Resources, Project administration. **Ivan Vokřál:** Supervision, Methodology, Investigation. **Karolína Štěrbová:** Methodology, Investigation, Data curation. **Ondřej Vosála:** Investigation, Data curation. **Beate Lungerich:** Methodology, Investigation. **Thomas Kurz:** Writing – review & editing, Supervision, Conceptualization. **Robin B. Gasser:** Writing – review & editing, Supervision. **Karel Harant:** Validation, Methodology, Formal analysis. **Lenka Skálová:** Writing – review & editing, Supervision, Conceptualization.

Ethics approval

All experimental procedures involving sheep were evaluated and approved by the Ethics Committee of the Ministry of Education, Youth and Sports of the Czech Republic (Project number MSMT-20144/2023–4) or in accordance with the Institutional Animal Ethics Guidelines (permit no. 23983; University of Melbourne) and Australian regulations.

Data availability

The mass spectrometry proteomics data have been deposited to the ProteomeXchange Consortium via the PRIDE (63) partner repository with the dataset identifier PXD059717. Other data are available at Zenodo repository at: https://doi.org/10.5281/zenodo.14697360.

Funding

Research in Hradec Králové was supported by Charles University project SVV 260664. PM and KŠ were supported by the project New Technologies for Translational Research in Pharmaceutical Sciences/NETPHARM, project ID CZ.02.01.01/00/22_008/0004607, co-funded by the European Union. Research in Melbourne was supported through grants LP220200614 and LP180101085 (to RBG) from the Australian Research Council linked to Phylumtech S.A. or Oz Omics Pty Ltd.

Declaration of interests

The authors declare that they have no known competing financial interests or personal relationships that could have appeared to influence the work reported in this paper.

Appendix A. Supplementary data

Supplementary data to this article can be found online at https://doi.org/10.1016/j.ijpddr.2025.100599.

References

Ahmad, N., Khan, S.A., Majid, H.A., Ali, R., Ullah, R., Bari, A., Akbar, N.U., Majid, A., 2024. Epidemiology and phylogeny of *Haemonchus contortus* through internal transcribed spacer 2 gene in small ruminants. Front. Vet. Sci. 11, 1380203. https://doi.org/10.3389/fvets.2024.

Arsenopoulos, K.V., Fthenakis, G.C., Katsarou, E.I., Papadopoulos, E., 2021. Haemonchosis: a challenging parasitic infection of sheep and goats. Animals 11. https://doi.org/10.3390/ani11020363.

Bertani, G., 1951. Studies on lysogenesis. I. The mode of phage liberation by lysogenic *Escherichia coli*. Bacteriol 62 (3), 293–300. https://doi.org/10.1128/jb.62.3.293-300.1951.

Brenner, S., 1974. Genetics of *Caenorhabditis elegans*. Genetics (Austin, Tex.) 77 (1), 71–94. https://doi.org/10.1093/genetics/77.1.71.

Brinzer, R.A., Winter, A.D., Page, A.P., 2024. The relationship between intraflagellar transport and upstream protein trafficking pathways and macrocyclic lactone resistance in *Caenorhabditis elegans*. G3 (Bethesda) 14 (3), jkae009. https://doi.org/10.1093/g3journal/jkae009.

Cai, E.J., Wu, R.Z., Wu, Y.H., Gao, Y., Zhu, Y.P., Li, J., 2024. A systematic review and meta-analysis on the current status of anthelmintic resistance in equine nematodes: a global perspective. Mol. Biochem. Parasitol. 257. https://doi.org/10.1016/j.molbiopara.2023.111600.

Davis, P., Zarowiecki, M., Arnaboldi, V., Becerra, A., Cain, S., Chan, J., Chen, W.J., Cho, J., da Veiga Beltrame, E., Diamantakis, S., Gao, S., Grigoriadis, D., Grove, C.A., Harris, T.W., Kishore, R., Le, T., Lee, R.Y.N., Luypaert, M., Müller, H.M., Nakamura, C., Nuin, P., Paulini, M., Quinton-Tulloch, M., Raciti, D., Rodgers, F.H., Russell, M., Schindelman, G., Singh, A., Stickland, T., Van Auken, K., Wang, Q.,

Williams, G., Wright, A.J., Yook, K., Berriman, M., Howe, K.L., Schedl, T., Stein, L., Sternberg, P.W., 2022. WormBase in 2022-data, processes, and tools for analyzing *Caenorhabditis elegans*. Genetics (Austin, Tex.) 220 (4), iyac003. https://doi.org/10.1093/genetics/iyac003.

Gasser, R.B., Bott, N.J., Chilton, N.B., Hunt, P., Beveridge, I., 2008. Toward practical, DNA-based diagnostic methods for parasitic nematodes of livestock–bionomic and biotechnological implications. Biotechnol. Adv. 26 (4), 325–334. https://doi.org/10.1016/j.biotechadv.2008.03.003.

Hahnel, S.R., Dilks, C.M., Heisler, I., Andersen, E.C., Kulke, D., 2020. *Caenorhabditis elegans* in anthelmintic research - old model, new perspectives. Int J Parasitol Drugs Drug Resist 14, 237–248. https://doi.org/10.1016/j.ijpddr.2020.09.005.

Harris, G., Wu, T., Linfield, G., Choi, M.K., Liu, H., Zhang, Y., 2019. Molecular and cellular modulators for multisensory integration in *C. elegans*. PLoS Genet. 15 (3), e1007706. https://doi.org/10.1371/journal.pgen.1007706.

Hughes, C.S., Moggridge, S., Muller, T., Sorensen, P.H., Morin, G.B., Krijgsveld, J., 2019. Single-pot, solid-phase-enhanced sample preparation for proteomics experiments. Nat. Protoc. 14 (1), 68–85. https://doi.org/10.1038/s41596-018-0082-x.

Jones, D.T., Taylor, W.R., Thornton, J.M., 1992. The rapid generation of mutation data matrices from protein sequences. Comput. Appl. Biosci. 8 (3), 275–282. https://doi.org/10.1093/bioinformatics/8.3.275.

Jumper, J., Evans, R., Pritzel, A., Green, T., Figurnov, M., Ronneberger, O., Tunyasuvunakool, K., Bates, R., Žídek, A., Potapenko, A., Bridgland, A., Meyer, C., Kohl, S.A.A., Ballard, A.J., Cowie, A., Romera-Paredes, B., Nikolov, S., Jain, R., Adler, J., Back, T., Petersen, S., Reiman, D., Clancy, E., Zielinski, M., Steinegger, M., Pacholska, M., Berghammer, T., Bodenstein, S., Silver, D., Vinyals, O., Senior, A.W., Kavukcuoglu, K., Kohli, P., Hassabis, D., 2021. Highly accurate protein structure prediction with AlphaFold. Nature 596, 583–589. https://doi.org/10.1038/s41586-021-03819-2.

Kamalian, L., Chadwick, A.E., Bayliss, M., French, N.S., Monshouwer, M., Snoeys, J., Park, B.K., 2015. The utility of HepG2 cells to identify direct mitochondrial dysfunction in the absence of cell death. Toxicol. Vitro 29 (4), 732–740. https://doi.org/10.1016/j.tiv.2015.02.011.

Kamath, R.S., Fraser, A.G., Dong, Y., Poulin, G., Durbin, R., Gotta, M., Kanapin, A., Le Bot, N., Moreno, S., Sohrmann, M., Welchman, D.P., Ziperlen, P., Ahringer, J., 2003. Systematic functional analysis of the *Caenorhabditis elegans* genome using RNAi. Nature 421 (6920), 231–237. https://doi.org/10.1038/nature01278.

Kellerová, P., Navrátilová, M., Nguyen, L.T., Dimunová, D., Raisová Stuchlíková, L., Štěrbová, K., Skálová, L., Matoušková, P., 2020. UDP-Glycosyltransferases and albendazole metabolism in the juvenile stages of *Haemonchus contortus*. Front. Physiol. 11, 594116. https://doi.org/10.3389/fphys.2020.594116.

Klauck, V., Pazinato, R., Lopes, L.S., Cucco, D.C., de Lima, H.L., Volpato, A., Radavelli, W.M., Stefani, L.C.M., da Silva, A.S., 2014. *Trichostrongylus* and *Haemonchus* anthelmintic resistance in naturally infected sheep from southern Brazil. Brazil An Acad Bras Cienc 86 (2), 777–784.

Kotze, A.C., Prichard, R.K., 2016. Anthelmintic resistance in *Haemonchus contortus*: history, mechanisms and diagnosis. Adv. Parasitol. 93, 397–428. https://doi.org/10.1016/bs.apar.2016.02.012.

Kulak, N.A., Pichler, G., Paron, I., Nagaraj, N., Mann, M., 2014. Minimal, encapsulated proteomic-sample processing applied to copy-number estimation in eukaryotic cells. Nat. Methods 11, 319–324. https://doi.org/10.1038/nmeth.2834.

Kulak, N.A., Geyer, P.E., Mann, M., 2017. Loss-less nano-fractionator for high sensitivity, high coverage proteomics. Mol. Cell. Proteomics 16 (4), 694–705. https://doi.org/10.1074/mcp.O116.065136.

Laing, R., Kikuchi, T., Martinelli, A., Tsai, I.J., Beech, R.N., Redman, E., Holroyd, N., Bartley, D.J., Beasley, H., Britton, C., Curran, D., Devaney, E., Gilabert, A., Hunt, M., Jackson, F., Johnston, S.L., Kryukov, I., Li, K., Morrison, A.A., Reid, A.J., Sargison, N., Saunders, G.I., Wasmuth, J.D., Wolstenholme, A., Berriman, M., Gilleard, J.S., Cotton, J.A., 2013. The genome and transcriptome of *Haemonchus contortus*, a key model parasite for drug and vaccine discovery. Genome Biol. 14 (8), R88. https://doi.org/10.1186/gb-2013-14-8-r88.

Lanusse, C., Canton, C., Virkel, G., Alvarez, L., Costa, L., Lifschitz, A., 2018. Strategies to optimize the efficacy of anthelmintic drugs in ruminants. Trends Parasitol. 34 (8), 664–682. https://doi.org/10.1016/j.pt.2018.05.005.

Le, T.G., Kundu, A., Ghoshal, A., Nguyen, N.H., Preston, S., Jiao, Y.Q., Ruan, B.F., Xue, L., Huang, F., Keiser, J., Hofmann, A., Chang, B.C.H., Garcia-Bustos, J., Jabbar, A., Wells, T.N.C., Palmer, M.J., Gasser, R.B., Baell, J.B., 2018. Optimization of novel 1-methyl-1*H* pyrazole-5-carboxamides leads to high potency larval development inhibitors of the barber's pole worm. J. Med. Chem. 61 (23), 10875–10894. https://doi.org/10.1021/acs.jmedchem.8b01544.

Le, T., Žárský, V., Nývltová, E., Rada, P., Harant, K., Vancová, M., Verner, Z., Hrdý, I., Tachezy, J., 2020. Anaerobic peroxisomes in *Mastigamoeba balamuthi*. roc Natl Acad Sci U S A 117 (4), 2065–2075. https://doi.org/10.1073/pnas.1909755117.

Liu, Y., Yang, X., Gan, J., Chen, S., Xiao, Z.X., Cao, Y., 2022. CB-Dock2: improved protein-ligand blind docking by integrating cavity detection, docking and homologous template fitting. Nucleic Acids Res. 50 (W1), W159–W164. https://doi.org/10.1093/nar/gkac394.

Mateus, A., Kurzawa, N., Perrin, J., Bergamini, G., Savitski, M.M., 2022. Drug target identification in tissues by thermal proteome profiling. Annu. Rev. Pharmacol. Toxicol. 62, 465–482. https://doi.org/10.1146/annurev-pharmtox-052120-013205.

McRae, K.M., McEwan, J.C., Dodds, K.G., Gemmell, N.J., 2014. Signatures of selection in sheep bred for resistance or susceptibility to gastrointestinal nematodes. BMC Genom. 15 (1), 637. https://doi.org/10.1186/1471-2164-15-637.

Mukherjee, A., Kar, I., Patra, A.K., 2023. Understanding anthelmintic resistance in livestock using "omics" approaches. Environ. Sci. Pollut. Res. Int. 30 (60), 125439–125463. https://doi.org/10.1007/s11356-023-31045-y.

Ng'etich, A.I., Amoah, I.D., Bux, F., Kumari, S., 2024. Anthelmintic resistance in soil-transmitted helminths: one-Health considerations. Parasitol. Res. 123 (1), 62. https://doi.org/10.1007/s00436-023-08088-8.

Nguyen, L.T., Kurz, T., Preston, S., Brueckmann, H., Lungerich, B., Herath, H., Koehler, A.V., Wang, T., Skálová, L., Jabbar, A., Gasser, R.B., 2019. Phenotypic screening of the "Kurz-box' of chemicals identifies two compounds (BLK127 and HBK4) with anthelmintic activity in vitro against parasitic larval stages of *Haemonchus contortus*. Parasites Vectors 12 (1), 191. https://doi.org/10.1186/s13071-019-3426-7.

Nguyen, L.T., Zajíčková, M., Mašátová, E., Matoušková, P., Skálová, L., 2021. The ATP bioluminescence assay: a new application and optimization for viability testing in the parasitic nematode *Haemonchus contortus*. Vet. Res. 52 (1), 124. https://doi.org/10.1186/s13567-021-00980-4.

Packer, J.S., Zhu, Q., Huynh, C., Sivaramakrishnan, P., Preston, E., Dueck, H., Stefanik, D., Tan, K., Trapnell, C., Kim, J., Waterston, R.H., Murray, J.I., 2019. A lineage-resolved molecular atlas of *C. elegans* embryogenesis at single-cell resolution. Science 365 (6459), eaax1971. https://doi.org/10.1126/science.aax1971.

Perrin, J., Werner, T., Kurzawa, N., Rutkowska, A., Childs, D.D., Kalxdorf, M., Poeckel, D., Stonehouse, E., Strohmer, K., Heller, B., Thomson, D.W., Krause, J., Becher, I., Eberl, H.C., Vappiani, J., Sevin, D.C., Rau, C.E., Franken, H., Huber, W., Faelth-Savitski, M., Savitski, M.M., Bantscheff, M., Bergamini, G., 2020. Identifying drug targets in tissues and whole blood with thermal-shift profiling. Nat. Biotechnol. 38 (3), 303–308. https://doi.org/10.1038/s41587-019-0388-4.

Piao, X.X., Sun, M., Yi, F.P., 2020. Evaluation of nematocidal action against *Caenorhabditis elegans* of essential oil of flesh fingered citron and its mechanism. J. Chem. 2020, 1–9. https://doi.org/10.1155/2020/1740938.

Pramanik, A., Anisuzzaman, Islam, P., Sachi, S., Islam, M.Z., Shohana, N.N., Rafiq, K., 2024. Saga of anthelmintic resistance: mechanisms of development, methods of detection and ways of mitigation. Ann. Anim. Sci. https://doi.org/10.2478/aoas-2024-0118.

Preston, S., Jabbar, A., Nowell, C., Joachim, A., Ruttkowski, B., Cardno, T., Hofmann, A., Gasser, R.B., 2015. Practical and low cost whole-organism motility assay: a step-by-step protocol. Mol. Cell. Probes 30 (1), 13–17. https://doi.org/10.1016/j.mcp.2015.08.005.

Preston, S., Jabbar, A., Gasser, R.B., 2016. A perspective on genomic-guided anthelmintic discovery and repurposing using *Haemonchus contortus*. Infect. Genet. Evol. 40, 368–373. https://doi.org/10.1016/j.meegid.2015.06.029.

Raisová Stuchlíková, L., Matoušková, P., Vokřál, I., Lamka, J., Szotáková, B., Sečkařová, A., Dimunová, D., Nguyen, L.T., Várady, M., Skálová, L., 2018. Metabolism of albendazole, ricobendazole and flubendazole in *Haemonchus contortus* adults: sex differences, resistance-related differences and the identification of new metabolites. Int. J. Parasitol. Drugs Drug Resist. 8 (1), 50–58. https://doi.org/10.1016/j.ijpddr.2018.01.005.

Redman, E., Packard, E., Grillo, V., Smith, J., Jackson, F., Gilleard, J.S., 2008. Microsatellite analysis reveals marked genetic differentiation between *Haemonchus contortus* laboratory isolates and provides a rapid system of genetic fingerprinting. Int. J. Parasitol. 38 (1), 111–122. https://doi.org/10.1016/j.ijpara.2007.06.008.

Roos, M.H., Otsen, M., Hoekstra, R., Veenstra, J.G., Lenstra, J.A., 2004. Genetic analysis of inbreeding of two strains of the parasitic nematode *Haemonchus contortus*. Int. J. Parasitol. 34 (1), 109–115. https://doi.org/10.1016/j.ijpara.2003.10.002.

Rychlá, N., Navrátilová, M., Kohoutová, E., Raisová Stuchlíková, L., Štěrbová, K., Krátký, J., Matoušková, P., Szotáková, B., Skálová, L., 2024. Flubendazole carbonyl reduction in drug-susceptible and drug-resistant strains of the parasitic nematode Haemonchus contortus: changes during the life cycle and possible inhibition. Vet. Res. 55 (1), 7. https://doi.org/10.1186/s13567-023-01264-9.

Sales, N., Love, S., 2016. Resistance of *Haemonchus* sp. to monepantel and reduced efficacy of a derquantel/abamectin combination confirmed in sheep in NSW, Australia. Vet. Parasitol. 228, 193–196. https://doi.org/10.1016/j.vetpar.2016.08.016.

Salle, G., Doyle, S.R., Cortet, J., Cabaret, J., Berriman, M., Holroyd, N., Cotton, J.A., 2019. The global diversity of *Haemonchus contortus* is shaped by human intervention and climate. Nat. Commun. 10 (1), 4811. https://doi.org/10.1038/s41467-019-12695-4.

Savitski, M.M., Reinhard, F.B.M., Franken, H., Werner, T., Savitski, M.F., Eberhard, D., Molina, D.M., Jafari, R., Dovega, R.B., Klaeger, S., Kuster, B., Nordlund, P., Bantscheff, M., Drewes, G., 2014. Tracking cancer drugs in living cells by thermal profiling of the proteome. Science 346 (6205), 1255784. https://doi.org/10.1126/science.1255784.

Schwarz, E.M., Korhonen, P.K., Campbell, B.E., Young, N.D., Jex, A.R., Jabbar, A., Hall, R.S., Mondal, A., Howe, A.C., Pell, J., Hofmann, A., Boag, P.R., Zhu, X.Q., Gregory, T., Loukas, A., Williams, B.A., Antoshechkin, I., Brown, C., Sternberg, P.W., Gasser, R.B., 2013. The genome and developmental transcriptome of the strongylid nematode *Haemonchus contortus*. Genome Biol. 14 (8), R89. https://doi.org/10.1186/gb-2013-14-8-r89.

Shanley, H.T., Taki, A.C., Nguyen, N., Wang, T., Byrne, J.J., Ang, C.S., Leeming, M.G., Nie, S., Williamson, N., Zheng, Y.T., Young, N.D., Korhonen, P.K., Hofmann, A., Chang, B.C.H., Wells, T.N.C., Häberli, C., Keiser, J., Jabbar, A., Sleebs, B.E., Gasser, R.B., 2024. Structure-activity relationship and target investigation of 2-aryl quinolines with nematocidal activity. Int J Parasitol Drugs Drug Resist 24, 100522. https://doi.org/10.1016/j.ijpddr.2024.100522.

Silverman, P.H., Campbell, J.A., 1959. Studies on parasitic worms of sheep in Scotland. I. Embryonic and larval development of *Haemonchus contortus* at constant conditions. Parasitology 49 (1–2), 23–38. https://doi.org/10.1017/s0031182000026688.

Sliwka, L., Wiktorska, K., Suchocki, P., Milczarek, M., Mielczarek, S., Lubelska, K., Cierpial, T., Lyzwa, P., Kielbasinski, P., Jaromin, A., Flis, A., Chilmonczyk, Z., 2016.

The comparison of MTT and CVS assays for the assessment of anticancer agent interactions. PLoS One 11 (5), e0155772. https://doi.org/10.1371/journal.pone.0155772.

Štěrbová, K., Rychlá, N., Matoušková, P., Skálová, L., Raisová Stuchlíková, L., 2023. Short-chain dehydrogenases in *Haemonchus contortus*: changes during life cycle and in relation to drug-resistance. Vet. Res. 54 (1), 19. https://doi.org/10.1186/s13567-023-01148-y.

Swiss, R., Niles, A., Cali, J.J., Nadanaciva, S., Will, Y., 2013. Validation of a HTS-amenable assay to detect drug-induced mitochondrial toxicity in the absence and presence of cell death. Toxicol. Vitro 27 (6), 1789–1797. https://doi.org/10.1016/j.tiv.2013.05.007.

Taki, A.C., Brkljaca, R., Wang, T., Koehler, A.V., Ma, G.X., Danne, J., Ellis, S., Hofmann, A., Chang, B.C.H., Jabbar, A., Urban, S., Gasser, R.B., 2020. Natural compounds from the marine brown alga *Caulocystis cephalornithos* with potent *in vitro*-activity against the parasitic nematode *Haemonchus contortus*. Pathogens 9 (7), 550. https://doi.org/10.3390/pathogens9070550.

Taki, A.C., Byrne, J.J., Wang, T., Sleebs, B.E., Nguyen, N., Hall, R.S., Korhonen, P.K., Chang, B.C.H., Jackson, P., Jabbar, A., Gasser, R.B., 2021. High-throughput phenotypic assay to screen for anthelmintic activity on *Haemonchus contortus*. Pharmaceuticals 14 (7), 616. https://doi.org/10.3390/ph14070616.

Taki, A.C., Wang, T., Nguyen, N.N., Ang, C.S., Leeming, M.G., Nie, S., Byrne, J.J., Young, N.D., Zheng, Y.T., Ma, G.X., Korhonen, P.K., Koehler, A.V., Williamson, N.A., Hofmann, A., Chang, B.C.H., Haeberli, C., Keiser, J., Jabbar, A., Sleebs, B.E., Gasser, R.B., 2022. Thermal proteome profiling reveals *Haemonchus* orphan protein HCO_011565 as a target of the nematocidal small molecule UMW-868. Front. Pharmacol. 13, 1014804. https://doi.org/10.3389/fphar.2022.1014804.

Taman, A., Azab, M., 2014. Present-day anthelmintics and perspectives on future new targets. Parasitol. Res. 113 (7), 2425–2433. https://doi.org/10.1007/s00436-014-3969-7.

Tamura, K., Stecher, G., Kumar, S., 2021. MEGA11: molecular evolutionary genetics analysis version 11. Mol. Biol. Evol. 38 (7), 3022–3027. https://doi.org/10.1093/molbev/msab120.

Tran, C.D., Timmins, P., Conway, B.R., Irwin, W.J., 2002. Investigation of the coordinated functional activities of cytochrome P450 3A4 and P-glycoprotein in limiting the absorption of xenobiotics in Caco-2 cells. J. Pharmacol. Sci. (Tokyo, Jpn.) 91 (1), 117–128. https://doi.org/10.1002/jps.1173.

van Wyk, J.A., Malan, F.S., 1988. Resistance of field strains of *Haemonchus contortus* to ivermectin, closantel, rafoxanide and the benzimidazoles in South Africa. Vet. Rec. 123 (9), 226–228. https://doi.org/10.1136/vr.123.9.226.

Veglia, F., 1915. The anatomy and life-history of the *Haemonchus contortus* (Rud.). Rep. Vet. Res. S. Afr. 3/4, 349–500.

Wang, Y., Yang, F., Gritsenko, M.A., Wang, Y., Clauss, T., Liu, T., Shen, Y., Monroe, M.E., Lopez-Ferrer, D., Reno, T., Moore, R.J., Klemke, R.L., Camp 2nd, D.G., Smith, R.D., 2011. Reversed-phase chromatography with multiple fraction concatenation strategy for proteome profiling of human MCF10A cells. Proteomics 11 (10), 2019–2026. https://doi.org/10.1002/pmic.201000722.

Yilmaz, E., Ramunke, S., Demeler, J., Krucken, J., 2017. Comparison of constitutive and thiabendazole-induced expression of five cytochrome P450 genes in fourth-stage larvae of *Haemonchus contortus* isolates with different drug susceptibility identifies one gene with high constitutive expression in a multi-resistant isolate. Int J Parasitol Drugs Drug Resist 7 (3), 362–369. https://doi.org/10.1016/j.ijpddr.2017.10.001.

Zajíčková, M., Nguyen, L.T., Skálová, L., Raisová Stuchlíková, L., Matoušková, P., 2020. Anthelmintics in the future: current trends in the discovery and development of new drugs against gastrointestinal nematodes. Drug Discov. Today 25 (2), 430–437. https://doi.org/10.1016/j.drudis.2019.12.007.

Zajíčková, M., Prchal, L., Navrátilová, M., Vodvárková, N., Matoušková, P., Vokřál, I., Nguyen, L.T., Skálová, L., 2021. Sertraline as a new potential anthelmintic against *Haemonchus contortus*: toxicity, efficacy, and biotransformation. Vet. Res. 52 (1), 143. https://doi.org/10.1186/s13567-021-01012-x.

Zajíčková, M., Prchal, L., Vokřál, I., Nguyen, L.T., Kurz, T., Gasser, R., Bednářová, K., Mičundová, M., Lungerich, B., Michel, O., Skálová, L., 2022. Assessing the anthelmintic candidates BLK127 and HBK4 for their efficacy on *Haemonchus contortus* adults and eggs, and their hepatotoxicity and biotransformation. Pharmaceutics 14 (4), 754. https://doi.org/10.3390/pharmaceutics14040754.

Zárybnický, T., Matoušková, P., Lancošová, B., Šubrt, Z., Skálová, L., Boušová, I., 2018. Inter-individual variability in acute toxicity of R-pulegone and R-menthofuran in human liver slices and their influence on miRNA expression changes in comparison to Acetaminophen. Int. J. Mol. Sci. 19 (6), 1805. https://doi.org/10.3390/ijms19061805.

Zheng, Y., Young, N.D., Song, J., Gasser, R.B., 2024. The mitogenome of the Haecon-5 strain of *Haemonchus contortus* and a comparative analysis of its nucleotide variation with other laboratory strains. Int. J. Mol. Sci. 25 (16), 8765. https://doi.org/10.3390/ijms25168765.